

PRECISE DETERMINATION OF THE $^{136}\text{Xe} - ^{136}\text{Ba}$ ATOMIC MASS
DIFFERENCE AND RELATED MASS DIFFERENCES IN Ba AND Cd

A Thesis

Submitted to the Faculty of Graduate Studies

University of Manitoba

In partial fulfillment

of the Requirements for the Degree:

Master of Science

by

Peter Michael McCowan

Winnipeg, Manitoba, Canada

© October, 2008

ACKNOWLEDGEMENTS

I would like to thank my supervisor, Dr. R.C. Barber, for his patience, support, knowledge, and encouragement over the years that I have been with the Atomic Mass Determinations group, and for introducing me to the world of Mass Spectroscopy.

In the past couple of years I have had the chance to meet and work with many exceptional individuals who helped me achieve my goals, and I would like to thank all of them: Richard Hamel, for the help in designing circuits, Grant Mollard, for his prompt and precise machining skills, Gilles Roy, for helping me in finding any needed material, instrument, or device, in the Allen Building catacombs, Adam Majer, for his impressive Linux programming skills, and Dr. K.S. Sharma for his helpful insight into the world of atomic mass measurements.

This work was supported by the Natural Sciences and Engineering Research Council of Canada. Without their support, this work would not exist.

And finally, I would like to sincerely thank all my friends and family, especially my father Rudi and mother Janet, for their caring, patience, and insurmountable support over the years.

Table of Contents

1 History of Mass Spectroscopy.....	1
1.1 History.....	1
1.2 Contributions of Mass Measurements to Nuclear Physics.....	3
1.3 Reaction and Decay Modes.....	3
1.4 Neutrinos and the Standard Model.....	5
1.4.1 The neutrino.....	5
1.4.2 Some Neutrino Mass Determination Experiments.....	6
1.4.3 Future Xenon Double Beta Decay Experiments.....	7
2 Double Focusing Theory.....	8
2.1 Ion Optics.....	8
2.2 Bleakney's Theorem.....	12
3 The Manitoba II Mass Spectrometer.....	14
3.1 The Ion Source.....	17
3.2 Electrostatic Analyzer (ESA).....	21
3.3 Magnetic Analyzer.....	21
3.4 The Collector and Detector Region.....	22
3.5 Recent Modifications to Manitoba II.....	22
3.5.1 The DDA and DSA.....	24
3.5.2 New Master Trigger Control Board.....	24
3.5.3 New Sawtooth Generator.....	25
3.5.4 Updated Source Voltage Switching.....	25
4 Experimental Procedures.....	31
4.1 Start-Up Procedures.....	31
4.2 Peak Matching.....	32
4.3 Computer Matching.....	33
4.4 Digital Acquisition.....	37
4.5 Data Analysis.....	37
5 Results.....	40
5.1 Motivation for the Measurement of $^{136}\text{Ba} - ^{136}\text{Xe}$.....	40
5.2 Experimental Details.....	40
5.3 Experimental Results.....	41
5.3.1 Discussion of Results.....	42

5.3.2 Implications of Results..... 43

References..... R-1

Appendix A – Circuits..... A-1

Appendix B – *Analyzer* (DSA) User Guide..... B-1

Appendix C – Relevant Program Codes..... C-1

C-1: *Analyzer* Source Code..... C-1

C-2: *Analyzer* Main Code..... C- 5

C-3: *Analyzer* Core Code..... C-13

Table of Figures

Ion Paths in a Magnetic and Electric Field Sector.....	11
Geometry of the Manitoba II Mass Spectrometer.....	15
Overall Control System.....	16
Physical Ion Source and Source Arm.....	18
Ion Source.....	19
Focusing and Steering Electrodes.....	20
Potentials, Delta-V Summing System, and Potentiometer.....	23
DDA Set-Up and DDA Module.....	26
DDA Data Capture Block Diagram.....	27
New Trigger Master Control.....	28
New Sawtooth Generator module.....	29
The Manitoba II.....	30
Master Timing Signals for the Manitoba II.....	34
Visual Matching.....	35
A Typical BAF Computer Match Configuration in AMDprime.....	36
DAMA ^{136}Xe energy Spectrum from Bernabei <i>et al.</i> (2003).....	45
DAMA Magnified ^{136}Xe energy Spectrum from Bernabei <i>et al.</i> (2003).....	46

Tables

Raw Data.....	41
Measured Doublets.....	42
Double Beta Decay Energies of ^{136}Xe	43

Abstract

In light of present (EXO) and future (BOREXINO & XMASS) projects searching for evidence of the, as yet, unobserved double-beta decay of ^{136}Xe , an atomic mass difference of $^{136}\text{Xe} - ^{136}\text{Ba}$ was determined using the high-precision Manitoba II mass spectrometer at the University of Manitoba. The Q-value for this difference was determined to be 2458.72(56) keV.

The double-beta decay mode can be either neutrino ($\beta\beta 2\nu$) or neutrinoless ($\beta\beta 0\nu$), where the latter would be proof of the Majorana nature of neutrinos. A $\beta\beta 0\nu$ decay, which violates several principles of the Standard Model of particle physics, would emit only electrons and would provide a defined peak at the Q-value for the decay. This decay would also require the Majorana neutrino to have a non-zero rest mass and be its own antiparticle.

Results of mass measurements on mass doublets of ^{135}Ba , ^{136}Ba , ^{137}Ba , and ^{138}Ba will be given. An improved measurement of the $^{116}\text{Cd}^{35}\text{Cl} - ^{114}\text{Cd}^{37}\text{Cl}$ doublet, previously done by Meredith *et al.* in 1973, will also be given.

Chapter 1

History of Mass Spectroscopy

1.1 History

Mass spectroscopy dates back to more than one hundred years ago involving experiments on the nature of matter in both the physical and chemical sciences. In the late 19th century, experiments studying gas discharge tubes led to the discovery of 'positive rays' (anode rays) by Goldstein. Goldstein's work formed a foundation for J.J. Thomson's work with the positive ray parabola apparatus [Th(1913)]. In Thomson's work, neon ions were deflected by a combined electric and magnetic field. His work suggested that neon was made up of two isotopes (two different atomic masses). Thomson's rays were separated according to mass thus making his instrument the first mass spectrometer.

In order to confirm the existence of isotopes among the lighter elements, Francis Aston, a student of Thomson, developed a mass spectrograph in 1919[As(1919)]. It was a combination of a separated electric and magnetic field, such that the ions first travelled through the electric field and then through the magnetic field, rather than simultaneously, as in Thomson's instrument. Aston did this to obtain a velocity focused beam; all ions of a specific e/m ratio, regardless of their speed, arrived at the same focused point. The apparatus, however, did not have any direction focusing; ions that diverge from the optic axis did not return to a focus. Aston compiled data on neon and chlorine and further confirmed the isotopic composition of the lighter elements. He later built a second, more refined, spectrograph with curved plates producing the electric field and a much larger and more powerful magnet. This allowed him to look at the heavy elements, notably Hg, in which 6 isotopes were discovered.

At the same time that Aston's first mass spectrograph was reported, A.J. Dempster [De(1918)] described an instrument that consisted of a 180° magnetic analyzer which inherently introduced direction focusing i.e. diverging monoenergetic ions at 0° will be focussed at 180°. Dempster collected data on Mg, Li, Ca, and Zn. He also discovered Uranium 235, an essential element of the atomic bomb.

Later, K.T. Bainbridge built an apparatus similar to Dempster's but added a velocity filter to remove the monoenergetic requirement of Dempster's set up [KB(1933)]. This filter involved an electric field and magnetic field which were tuned precisely so that the magnetic force and electric force were equal and opposite, allowing ions of different e/m ratios (energy) but the same speeds to pass through the filter.

Bainbridge studied elements in the lighter regions of the mass table, most notably heavy hydrogen.

All of the above mass spectrographs possessed either direction or velocity focusing, but never both. It was recognized at this point that an instrument that combined both would be desirable.

A full mathematical analysis of ion optics was given by Herzog in 1934. He derived a system of equations that described the mechanics of ions travelling through uniform magnetic and radial electrostatic fields [He(1934)]. With these equations, one could derive many geometrical arrangements which would produce double focusing. Thereafter, double focusing machines were built by Dempster, Bainbridge, J. Mattauch, R. Herzog, A.O. Nier, and others, all independent of each other [Du(1986)]. Other advances were made in vacuum techniques and electronics, over the following years, which led to a steady increase in the precision with which a peak could be located.

The equations of Herzog ignore higher order image aberrations. During the 1950's, Hintenberger and König considered these and gave a compilation of specific geometrical arrangements for double focusing instruments that would cancel out higher order aberrations [Hi(1959)]. One of these geometrical arrangements was used for the construction of Manitoba II.

These first order theories also ignore magnetic and electric fringe field effects. This was discussed in great detail by Coggeshall [Co(1947)]. König and Hintenberger [KoH(1955)] then suggested using a 'shim' adjacent to the poles of the magnet to provide an abrupt termination of the fringe fields. The solution for the instrument used in this work is discussed in §3.3.

The desire to obtain more precise measurements of the masses of stable nuclides led to the development of instruments having greatly improved resolution and precision. Over the next couple of decades, double focusing instruments led the way in this work.

Recently, Penning ion traps have been used to make precise atomic mass measurements. These devices confine charged particles by using a constant static magnetic field and a spatially inhomogeneous static electric field. Determining the cyclotron frequency of ions in these fields with high precision, and knowing the magnitude of the magnetic field, along with the charge of the ion, the mass can be determined very precisely (up to a couple parts in 10^{-10} , for example see [Re(2007)]). It is also used to very accurately determine atomic masses of unstable isotopes [Sh(1995,1998)]. Penning traps are very efficient with ion use as they need much less than the constant supply of ions that a double focusing instrument requires [Sa(2004)].

1.2 Contributions of Mass Measurements to Nuclear Physics

Precision in accumulated atomic mass data is important to nuclear physics. The mass of a neutral atom may be expressed as:

$${}^A_Z M = Z(m_p + m_e) + N m_n - BE_{\text{nucleus}} - BE_{\text{electrons}} \quad (1-1)$$

where Z is the atomic number (number of protons), N is the mass number, A is the atomic mass number (nucleon number), m_p , m_e , and m_n are masses of the proton, electron, and neutron respectively, and BE is the Binding energy. Since the BE_{nucleus} is much larger than the $BE_{\text{electrons}}$, the mass effectively reflects the BE_{nucleus} , and gives information about the nuclear structure such as nuclear shells or changes in nuclear shape.

Mass measurements with a deflection mass spectrometer are always made by measuring the relatively small mass differences between members of a mass “doublet”. Nuclear reactions are of the form:



The reaction energy, Q , may appear as kinetic energy of the product particles, emission of gamma rays, or metastable energy that may remain in the nucleus. X-rays may also be emitted but are due to the new nucleus having a different atomic number and hence a different number of electrons. The new electronic configuration must adjust to the lowest energy levels, a process which produces low energy X-rays. Decay reactions such as alpha decay, beta decay, and neutron-gamma reactions are discussed in §1.3. Since $E = mc^2$, one gets a mass difference from nuclear reactions (of all types in principle).

All the accumulated mass data in the last 100 years has been compiled and/or updated into the Atomic Mass Table. Each datum can be treated as a linear equation with an associated error involving two or more masses. When all of the data from mass spectroscopic doublets, nuclear reactions, and decays are included we have an over determined set of equations linking the masses (which are the unknowns). A least squares adjustment is the appropriate method of deriving the ‘best’ values for the masses and was first introduced by Mattauch [Ma(1960)]. The 2003 Atomic Mass Evaluation [Au(2003)] is the latest such compilation of these adjusted values.

1.3 Reaction and Decay Modes

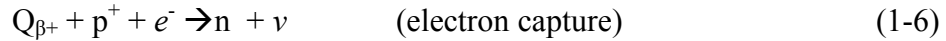
With nuclear reactions one can have a nuclear decay, which is the process whereby an unstable nucleus loses energy by emitting radiation. The radiation can be particles and/or electromagnetic waves. Alpha, beta, and gamma decay are the important contributors to atomic mass evaluations.

Alpha decay involves the nucleus ejecting two protons and two neutrons as a bound particle, called an alpha particle, which is the nucleus of the He atom. A typical alpha decay equation looks like:



Here ${}^{238}\text{U}$ decays to ${}^{234}\text{Th}$ via an alpha decay. Q is the energy that is released in the decay. The mass of the alpha particle is known precisely, so the mass difference between the parent and daughter nuclei can be easily determined by measuring Q . Conversely Q can be calculated accurately if the parent and daughter nuclei masses are well known. The energy Q consists of the kinetic energy of the alpha particle plus the kinetic energy of the recoil nucleus. The kinetic energy of the alpha particle can be measured quite accurately using magnetic analyzers or solid state detectors.

Another type of decay known as beta decay takes place in two ways. In negative beta decay the nucleus converts a neutron into a proton and then emits an electron and an antineutrino. In positive beta decay, energy is required to convert a proton into a neutron and emits a positron and neutrino. The equations for beta-decays are:



Taking the entire atom into consideration, we see that the beta minus decay is:



where,

$$Q_{\beta^-} = {}^A_Z\text{X} - {}^A_{Z+1}\text{Y} \quad (1-8)$$

Here ν is the symbol for a neutrino and $\bar{\nu}$ is for an antineutrino. Q_{β^-} is the energy released during the decay and is the maximum kinetic energy of the electron and neutrino. For this experiment we are interested in the double beta decay.

Double beta decay ($2\nu\beta\beta$) occurs as well and the output, along with the daughter nucleus, is just doubled (two electrons two antineutrinos). Double beta decay can also be neutrinoless ($0\nu\beta\beta$). The $0\nu\beta\beta$ decay can provide important information on the nature of the neutrino, on its Majorana mass, and on possible right-handed components in the leptonic currents. Theoretically ($0\nu\beta\beta$) can emit two majorana neutrinos or no neutrinos at all.

Electron capture is the process where the nucleus absorbs an orbiting electron and emits one neutrino. The daughter nucleus produced from this capture is left in an excited but unstable state. In principle, one can also have a double electron capture as well as have an electron capture and a positron emission where one positron and two neutrinos are emitted.

For electron capture, or ‘K-capture’, the electron is captured from the innermost orbit, the K-shell (L-capture also exists), and the corresponding expression is:

$${}^A_Z X \rightarrow {}^A_{Z-1} Y + \nu + Q_{K^+} \quad (1-9)$$

where,

$$Q_{K^+} = {}^A_Z X - {}^A_{Z-1} Y \quad (1-10)$$

For β^+ emission we have,

$$Q_{\beta^+} = {}^A_Z X - {}^A_Y + e^+ + \nu \quad (1-11)$$

One should notice that Q_{β^+} has to exceed $2(m_e c^2)$ for the decay to proceed with β^+ emission. Since the final state has an electron removed rather than a positron added, electron capture is energetically favored by $2m_e c^2$, for low-energy decays.

Another type of reaction, denoted by (n, γ) , known as a neutron capture is the process by which a target nucleus absorbs a neutron and emits a gamma ray. The energy of the gamma ray given off may be determined with very good precision (~ 0.04 to 0.2 keV) with Ge (Li) solid state detectors. Such reactions comprise a significant body of precise mass difference data.

1.4 Neutrinos and the Standard Model

1.4.1 The Neutrino

A neutrino is a fermion (obeys Fermi-Dirac statistics) that travels at speeds close to the speed of light. It has a rest mass is very small compared to the electron mass. A neutrino can pass through ordinary matter virtually undetected. There are three known types of neutrinos that exist in nature: the electron-neutrino, the muon-neutrino, and the tau-neutrino (all of which have their accompanying antineutrino). Their name comes from their partner leptons in the Standard Model of particle physics. In double beta-decay we are interested in the electron-(anti)neutrinos. In principle, knowing the nuclear mass data, one can calculate the energies lost or gained in a decay and the left over energy (mass) can be attributed to a neutrino(s).

A yet unseen, but possible decay mode is neutrinoless double-beta decay. For this type of decay all of the available energy is shared by the two β particles. Neutrinoless beta decay would violate the standard model and is therefore of great interest. If neutrinoless decay is observed it would prove the Majorana nature of neutrinos. A Majorana particle is a fermion that is its own antiparticle and therefore has a non-zero rest mass.

The double beta decay candidate studied in this experiment is ^{136}Xe , which decays to ^{136}Ba . Recent studies have shown that this decay may very well be a neutrinoless decay [Al(1988), Vu(1993), EXO(2006), Be(2003)].

A typical beta decay with its lepton family conservation looks like:

$$n \rightarrow p^+ + e^- + \bar{\nu} \quad (1-12)$$

$$L_e : 0 = 0 + 1 + -1$$

Here the lepton number is conserved and the standard model holds (the neutron and proton are baryons). If no neutrinos were produced, there would be a violation in the model, and an appropriate amendment to the Standard Model would be required for this type of decay.

Recent data from both the SNO observatory [Ah(2002), Os(2003)] and the Super-Kamiokande Collaboration [Fu(1998)] have confirmed that solar neutrinos oscillate in flavor (i.e. a muon neutrino can change to a tau neutrino, and an electron neutrino oscillates into a muon neutrino. These oscillations can occur multiple times). As a corollary of neutrino oscillations, $(0\nu\beta\beta)$ decay can choose between the two mass hierarchies for a Majorana neutrino. These oscillations are also confirmation that neutrinos have mass.

1.4.2 Some Neutrino Mass Determination Experiments

The Mainz neutrino mass experiment is investigating the tritium β decay spectrum to determine a mass for the electron antineutrino. They have recently provided an upper limit to the electron antineutrino where $\langle m_{\nu e} \rangle < 2.2\text{eV}$ [We(1999)]. To date this is the most accurate upper limit.

The Milano Experiment reported an effective Majorana neutrino mass with an upper limit of 13.3eV [Al(1988)].

Using a Xe time projection chamber, located at the Gotthard underground laboratory, an upper limit of the effective Majorana neutrino mass was found to be 2.2 eV [Vu(1993)].

Detecting neutrinos from the supernova 1987A, in the Large Magellanic Cloud, using the Kamiokande-II collaboration and the IMB collaboration, placed an upper limit on the electron neutrino to be $\langle m_{\nu e} \rangle < 11\text{eV}$ [Ba(1987)].

Geochemical measurements involving the neutrinoless double beta decay of ^{128}Te and ^{130}Te give an upper limit of $\langle m_{\nu e} \rangle < 0.44\text{eV}$ [Ki(1983)].

The Heidelberg-Moscow experiment studied the double beta decay of ^{76}Ge and found an upper limit to the effective mass of the Majorana-neutrino to be $< 0.20\text{eV}$ [KI(2001)]. This is less than but within the range of values estimated from Hykway, $\langle m_{\nu m} \rangle < 1.63\text{eV}$ to $< 0.99\text{eV}$, based on his insertion of the ^{76}Ge decay Q value [Hy(1999)].

1.4.3 Future Xenon Double Beta Decay Experiments

A current research project looking at the neutrinoless double beta decay of ^{136}Xe is the Enriched Xenon Observatory (EXO) [EXO(2006)]. EXO will use a multi-ton time projection chamber (TPC) of either high-pressure gas or liquid Xe. In this project the half-life of ^{136}Xe is measured and the related *effective neutrino mass* is calculated. The expected precision on this value is 0.01eV .

In 2008, the EXO project was moved to the U.S. Department of Energy's Waste Isolation Pilot Plant in New Mexico, which is 2150ft below the surface of the earth. This depth provides protection from cosmic rays and other earth surface radiation which introduce high background levels. Measurements are planned to commence in spring 2009.

The NEMO SuperNEMO project is currently looking at possible neutrinoless decay modes for ^{100}Mo , ^{82}Se , ^{116}Cd , ^{96}Zr , ^{150}Nd , ^{48}Ca , ^{136}Xe , and ^{130}Te [St(2008)]. The SuperNEMO project has not produced any results for Xe yet.

The BOREXINO project involves loading the liquid scintillator of the BOREXINO facilities with xenon, isotopically enriched in ^{136}Xe [Ca(2000)]. This project will not get underway for quite some time though due to a scintillator spill that contaminated the water outside the Gran Sasso Laboratory. If the project ever does get underway it is predicted that with 80% enriched ^{136}Xe , BOREXINO can achieve a half-life sensitivity of 1.14×10^{27} years or a neutrino mass $\langle m_{\nu} \rangle \sim 40\text{-}200\text{ meV}$.

The XMASS project utilizes a liquid Xe experiment with the goal of observing ^7Be solar neutrinos from the pp-chain in real time, direct-observation of Cold Dark Matter (CDM), and the observation and measurement of the $0\nu\beta\beta$ -decay of ^{136}Xe [Mo(2001)]. It is still in the research and development stage.

Chapter 2

Double Focusing Theory

2.1 Ion Optics

As mentioned in chapter 1 a double focusing instrument requires that ions travel through an electric and then a magnetic field. If an ion with charge q , and mass m_o , travels with a speed v_o , perpendicular to a magnetic field, B , then the centripetal force on the ion is provided by the magnetic force. That is:

$$\frac{m_o v_o^2}{r_m} = qv_o B \quad (2-1)$$

and the radius that the ion will travel through is:

$$r_m = \frac{m_o v_o}{qB} \quad (2-2)$$

The radius of curvature for the ion path in a radial electric field is:

$$r_e = \frac{2km_o v_o^2}{qV} \quad (2-3)$$

where V is the voltage across the cylindrical electrostatic analyzer plates, having a radius of $a+k$ and $a-k$ (with $k \ll a$).

A real ion source produces ions having a small spread in velocity, $v = v_o(1+\beta)$ and a small angular spread, 2α . With this realistic consideration, the trajectory of the ions through a magnet sector was described by Herzog [He(1934)]. Referring to fig. 2-1, ions of mass m , and velocity v , start from an object point O and an angular spread of 2α . The ions travel a distance of l_m' and enter the magnetic field perpendicular to the field lines. The magnetic force constrains the ions to travel in a radius of r_m through an angle of Φ_m until they leave the field, travel a distance of l_m'' , then focus at point I .

Herzog treated the optics like a prism plus cylindrical lens and expressed this in Newtonian form. He gave that the focal length of this 'magnetic lens' is:

$$f_m = \frac{r_m}{\sin \Phi_m} \quad (2-4)$$

and the object and image distances are given by:

$$(l_m' - g_m)(l_m'' - g_m) = f_m^2 \quad (2-5)$$

where $g_m = f_m \cos \Phi_m$.

If b_m' and b_m'' are the object and image width respectively then the magnification, ψ , is:

$$\frac{b_m''}{b_m'} = \frac{f_m}{l_m' - g_m} = \psi \quad (2-6)$$

If we now introduce small variations in the mass and velocity, i.e. $m = m_o(1+\gamma)$ and $v = v_o(1+\beta)$, where $\gamma, \beta \ll 1$, then the expression for the image width (paraxial approximation) is:

$$b_m'' = r_m (\beta + \gamma) \left[1 + \frac{f_m}{l_m' - g_m} \right] - b_m' \left(\frac{f_m}{l_m' - g_m} \right) \quad (2-7)$$

which can be simplified too [Sh(1979)],

$$b_m'' = r_m (\beta + \gamma)(1 + \psi) - b_m' \psi \quad (2-8)$$

where ψ is a constant of the magnet geometry only.

Now referring to fig. 2-2, with the Herzog notation, we get the equations for ions travelling through a radial electric field sector.

Again the image and object distances are given by:

$$(l_e' - g_e)(l_e'' - g_e) = f_e^2 \quad (2-9)$$

with,

$$f_e = \frac{r_e}{\sqrt{2} \sin(\sqrt{2}\Phi_e)} \quad (2-10)$$

$$g_e = f_e \cos(\sqrt{2}\Phi_e) \quad (2-11)$$

and the image displacement is given by,

$$b_e'' = r_e \left(\beta + \frac{1}{2} \gamma \right) \left[1 + \frac{f_e}{l_e' - g_e} \right] - b_e' \left(\frac{f_e}{l_e' - g_e} \right) \quad (2-12)$$

or,

$$b_e'' = r_e \left(\beta + \frac{1}{2} \gamma \right) (1 + \xi) - b_e' \xi \quad (2-13)$$

where again the constant ξ is defined only by the geometry of the electric field sector.

In order to achieve double focusing we consider an apparatus where we combine both fields. Here, the image produced by the electric field becomes the object for the magnetic field. Combining equations 2-13 with 2-8 we get:

$$b_m'' = r_m (\beta + \gamma) (1 + \psi) - \psi \left[r_e \left(\beta + \frac{1}{2} \gamma \right) (1 + \xi) - b_e' \xi \right] \quad (2-14)$$

For velocity focusing, the coefficient of $\beta = 0$; that is we get the following:

$$r_m [1 + \psi^{-1}] - r_e [1 + \xi] = 0 \quad (2-15)$$

Now choosing an object slit width of S_o , for the electrostatic analyzer, we see that two masses will just be resolved if the centres of the mass peaks equal MS_o , where M is the total magnification of the system, the detector plane is perpendicular to the ion beam, and photographic detection (which does not broaden the peak) is used.

For electrical detection, where the beam of width MS_o is swept across the detector slit, maximum sensitivity occurs when the detector slit width is equal to the beam width. This leads to a decrease in resolving power by a factor of 2. From these assumptions and from the above equations we find the resolution and dispersion respectively:

$$\frac{\Delta M}{M} = \frac{2S_o}{r_e} \left[\frac{\xi}{1 + \xi} \right] \quad (2-16)$$

$$d = \frac{r_m}{200} (1 + \psi), \text{ per } 1\% \text{ mass difference} \quad (2-17)$$

It is interesting and important to see that the resolution depends strictly on the geometry of the electrostatic analyser and the slit(s), while the dispersion depends only on the magnetic analyzer geometry. Also for a given electrostatic analyzer of radius r_e and angle Φ_e velocity focusing will only exist for one r_m and one Φ_m .

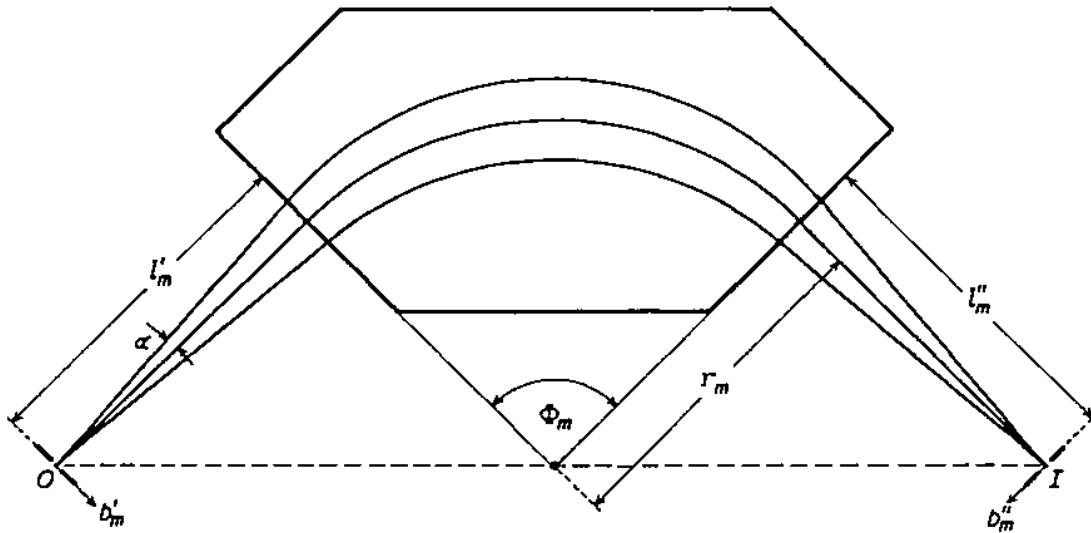


Fig.2-1 Ion Paths in a Magnetic Field Sector [Du(1986)]

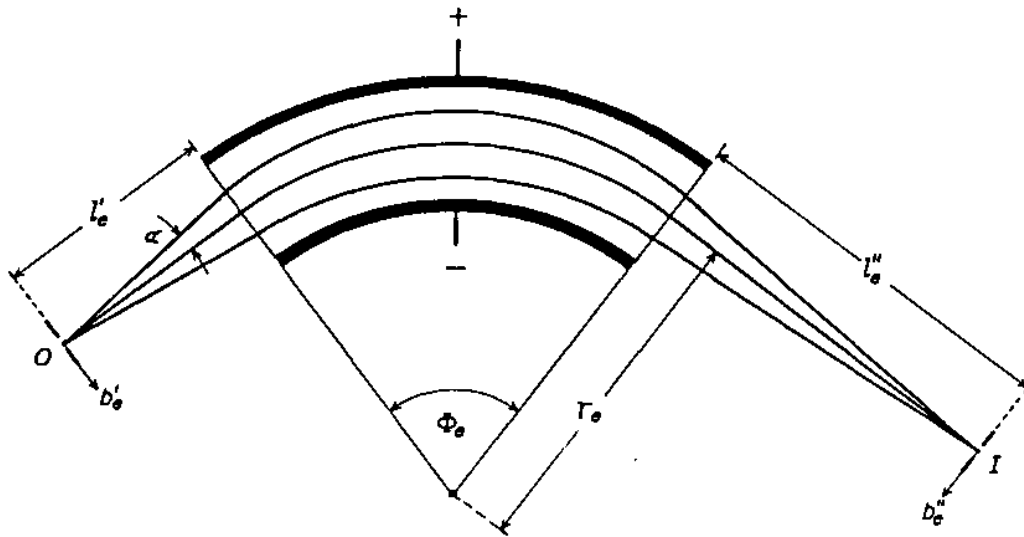


Fig.2-2 Ion Paths in an Electric Field Sector [Du(1986)]

Equations 2-16 and 2-17 were derived by neglecting fringe field effects for the magnetic and electric fields.

More generally the position of the beam at the detector plane, for an ion initially on the optic axis at the source slit, is:

$$y = r_m \{ B_1 \alpha_e + B_2 \beta + B_{11} \alpha_e^2 + B_{12} \alpha_e \beta_e + B_{22} \beta^2 \} \quad (2-18)$$

Using the notation of Duckworth *et al.* [Du(1986)], r_m is the radius of the magnet and hence the overall scale factor, α_e is the angular spread of the beam of ions at the ESA entrance from the axis, and β_e is the deviation of the ions velocity from v_0 . The Herzog theory gives the condition under which $B_1 = B_2 = 0$, that is first order double focusing.

During the 1950's the second order geometry was studied by Hintenberger and König [Hi(1959)]. The culmination of this work was a set of specific geometrical arrangements for double focusing instruments that produce second order focusing. One of these designs, chosen for its compact geometry, is the Manitoba II. Specifically, this instrument has an intermediate direction focus, straight magnetic field boundaries, and does not have large drift spaces where stray magnetic field can produce unwanted modulations of the beam position.

2.2 Bleakney's Theorem

As previously mentioned, mass measurements using a double-focusing mass spectrometer are always made by measuring relatively small mass differences between members of a mass "doublet". This is done, in simple terms, by changing a field(s) in order to move one mass peak to the position of the other member of the doublet. Considering the numerous electric and magnetic fields involved in directing ions from source to detector, one would hope to find a simple relation between a parameter change in *one* field, which is easily measurable, and would yield a matching condition for the doublet.

Bleakney considered a general combination of electric and magnetic fields [Bl(1936)]. He showed that two different masses, m_1 and m_2 , will have identical trajectories in an electromagnetic field, provided that the electric field is varied so that $m\mathbf{E}$ is a constant, while the magnetic field remains constant, ie.,

$$m_1 \mathbf{E}_1 = m_2 \mathbf{E}_2 \quad (2-19)$$

Since the applied voltage is directly related to the electric field of an electrostatic analyzer we have:

$$m_1 V_1 = m_2 V_2 \quad (2-20)$$

and

$$(M_L + \Delta M)V = M_H(V + \Delta V_L) \quad (2-21)$$

Hence,

$$\frac{\Delta M}{M_L} = \frac{\Delta V_L}{V} \quad (2-22)$$

where M_L is the lower mass of the doublet and ΔV_L is the voltage it needs to match the higher mass, M_H , of the doublet.

Chapter 3

The Manitoba II Mass Spectrometer

The Manitoba II is a high resolution, second order double focusing mass spectrometer. As mentioned in chapter 2 it was constructed from one of Hintenberger and König's designs from the late 1950's. Overall the goal of this design is to produce a high resolution image. In mass measurements, the location of the peak is determined; therefore the sharper the peak(s), the better this can be done. A diagram of the geometry and the dimensions of the ion path can be found in fig. 3-1 [Ba(1971)].

One wishes to use Bleakney's theorem for mass measurements. Therefore we have voltage switching and other precautions to make ions follow the same path. A simple block diagram of the voltage-mass measurement system is displayed in fig. 3-2. The ion path is insensitive to changes in the accelerating voltage V_a and the quadrupole voltage, but very sensitive, as discussed in §2.2, to the ΔV across the electrostatic analyzer (ESA) plates. The block diagram has changed a little in terms of potential devices and new digital devices, but its operation is basically unchanged. These changes will be discussed in the later sections.

The instrument is described in detail by Bishop [Bi(1969) & Bi(1970)] and Barber [Ba(1971)], with the important overall characteristics:

Accelerating potential	$V_a = 19.7\text{kV}$
Magnification	$M = -\frac{1}{2}$
Resolution ¹	$R \approx \frac{1}{250,000}$
Source Slit width (for best resolution)	$\approx 2\mu\text{m}$

In describing the Manitoba II apparatus, we will consider this in four parts: the ion source, the electrostatic analyzer, the magnetic analyzer, and the detector. The first three mentioned have remained substantially unchanged; the detector area and accompanying electronic devices have undergone upgrades during the work of D. Barillari [Ba(1999)] and the present work.

¹ The best resolution on this instrument was achieved by Koziar [Ko(1977)] where 1/500,000 was obtained for a single record (measured at 15% of the peak height), while well over 1/400,000 was obtained for a complete run of a Hg-Cl₂ doublet.

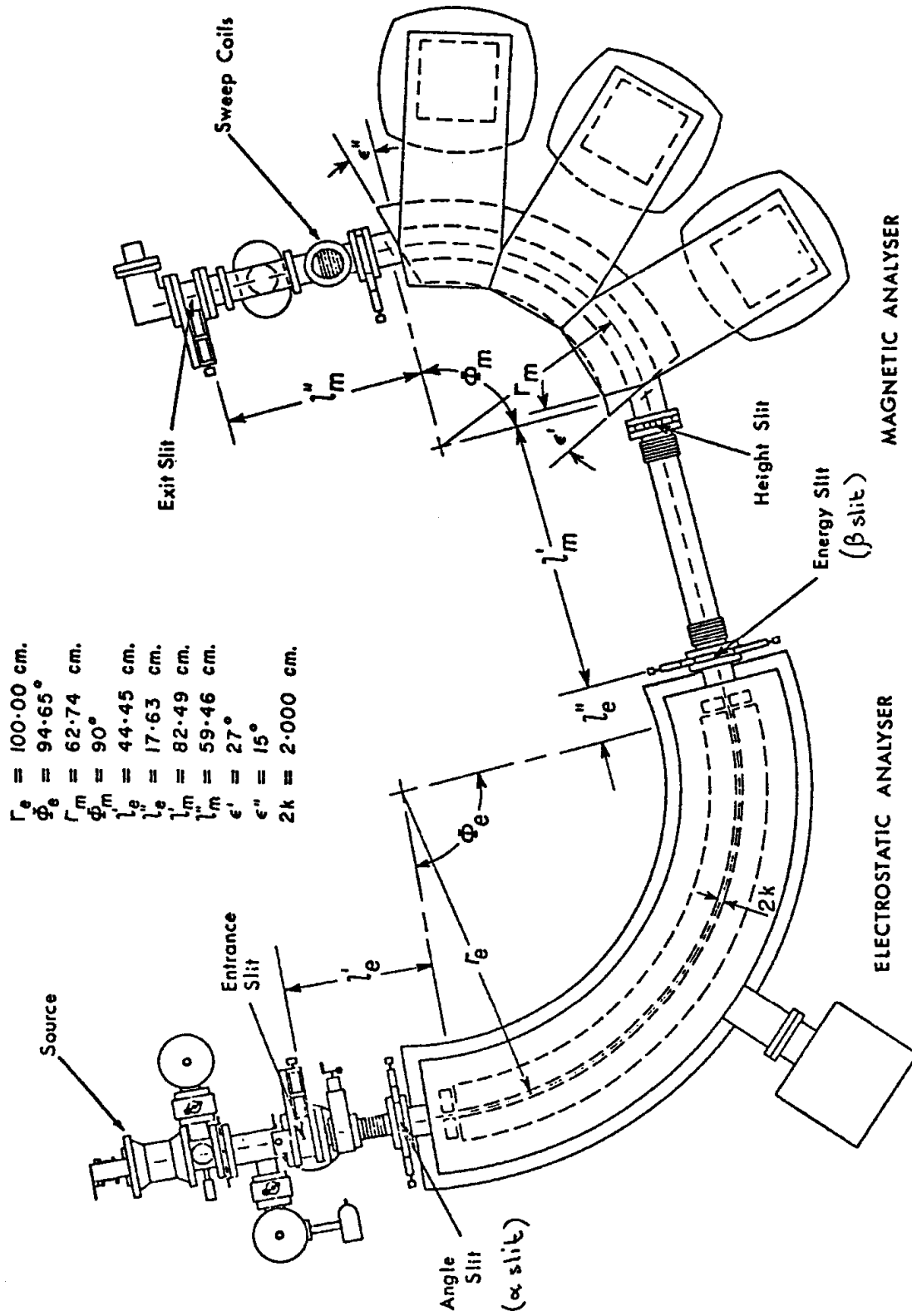


Figure 3-1 Geometry of the Manitoba II Mass Spectrometer

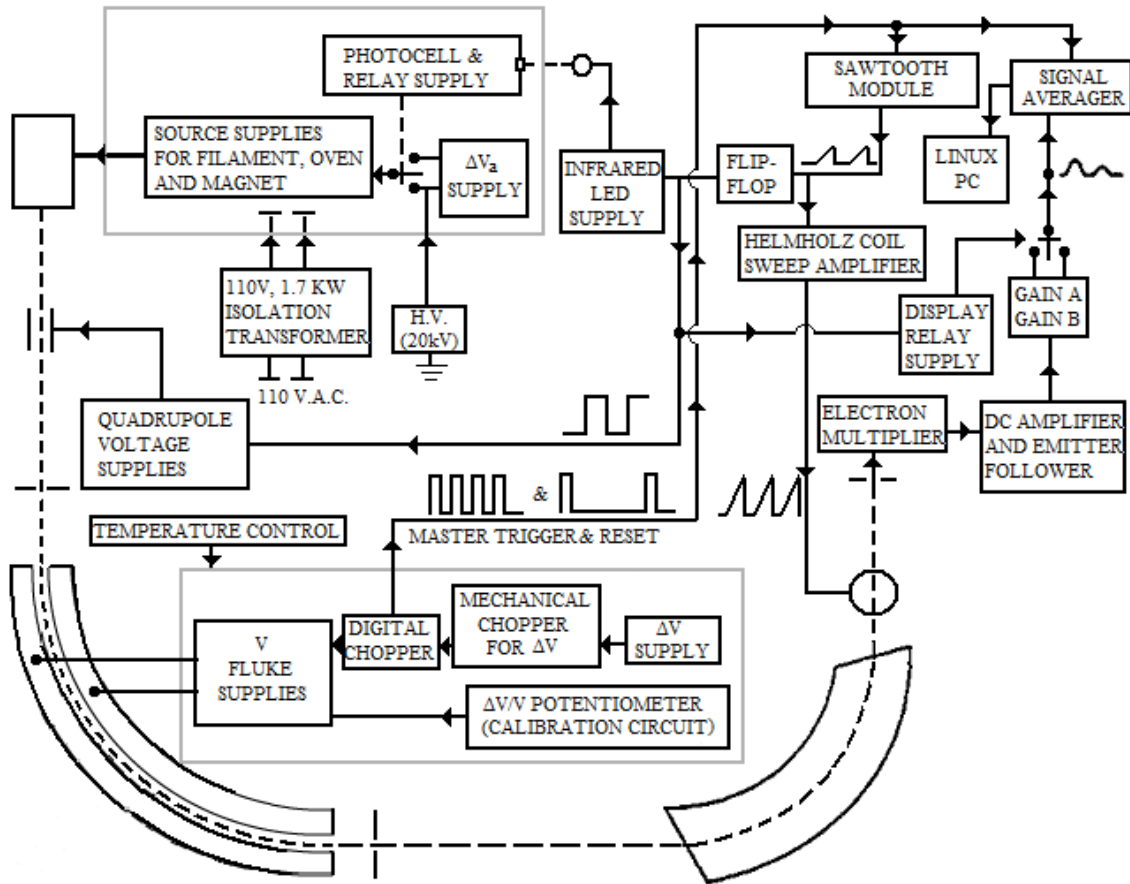


Fig. 3-2 Overall Control System [Ba(1971)]

3.1 The Ion Source

The ion source and source arm are pictured in fig.3-3 while a schematic of the ion source is seen in fig. 3-4. The source consists of an oven, a filament, a repeller pole, and a magnetic coil. The oven was a 6.35cm long tube of tantalum pressed together to have 0.32cm height of separation on the inside (from top to bottom), with a 0.08cm hole drilled transversely through the center. A larger hole in the oven's upper end was made to connect it to a gas feed through. Tantalum was chosen because it has a high melting point ($\sim 3000^{\circ}\text{C}$), and the BaCl_2 (boiling point $\sim 1560^{\circ}\text{C}$) required strong heating. The oven was coated with a layer of high-temperature sealing cement (Sauereisen 3 Tempseal cement), wrapped with Re ribbon, and coated once more with another layer of the sealing cement. The ribbon was connected to a current supply in order to heat the oven and sufficiently raise the vapour pressure of the BaCl_2 sample. The filament, also made of Re ribbon and slightly peaked in the middle, was centered below the 0.08cm hole of the oven. The repeller rod, made of iron and placed behind the filament (which is behind the oven), was at a negative potential and thus *repelled* the electrons that were emitted from the filament towards and into the oven. The magnetic coils produce an axial field which confines the electrons to a beam that passes into the oven.

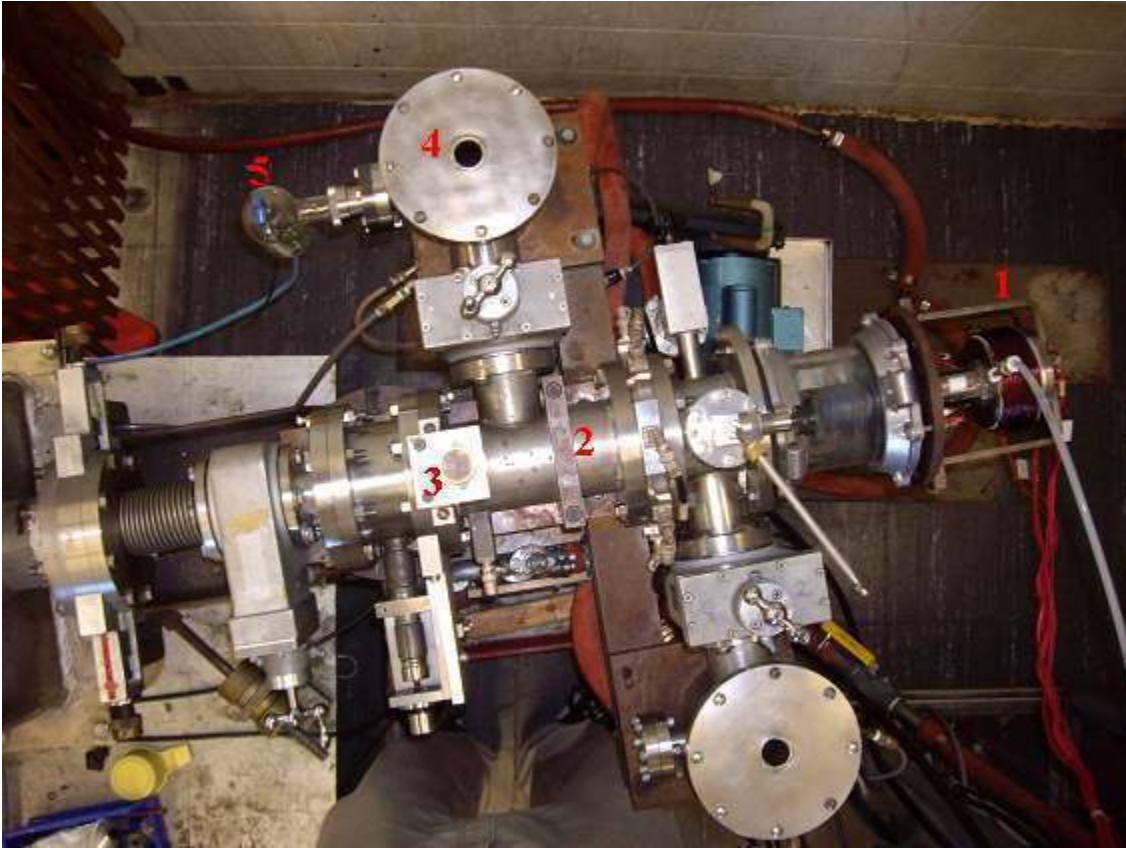
The sample molecules were introduced into the oven in either solid or gaseous form (via a needle valve) and then bombarded by electrons (from the heated Re filament) which ionized them. Since the whole body of the source is maintained at an accelerating potential of 19.7keV, positive ions are extracted from the source and accelerated toward the ESA.

The ions then pass through a pair of horizontal and vertical deflection plates, then through a double quadrupole lens. The deflection plates allow the user to steer the beam up/down and left/right, and the quadrupole lens permits the adjustment of the horizontal and vertical focus. Each pair of quadrupoles has opposite polarities, focusing the beam in one plane while defocusing it in another, i.e. the quadrupoles are arranged so that the pair can focus the beam on the principal slit (in the horizontal direction) while producing a parallel beam in the vertical direction.

The principal slit of the system is the object for the ESA and determines the resolving power of the instrument. A slit width of $2\mu\text{m}$ would produce a resolution of 1/300,000. In this experiment, the slit width was $\sim 2.5\text{-}3\mu\text{m}$ and the collector slit was $\sim 1.5\mu\text{m}$, yielding a resolution of roughly 1/225,000.

This part of the source arm can be seen in fig. 3-5. The pressure in this vacuum was $\sim 2 \times 10^{-6}$ Torr, depending on the ions being sampled, and was produced by two 150L/s diffusion pumps.

For practical adjustment of the focusing, the whole source (including ion source and source arm) can be physically moved in all three dimensions with respect to the ESA to obtain optimum alignment.



- 1-Ion Source
- 2-Source Arm (deflector plates & quadrupole lens)
- 3-Principal Slit
- 4-Diffusion Pump
- 5-Ion Gauge for Diffusion Pump

Fig.3-3 Physical Ion Source and Source Arm (as seen overhead)

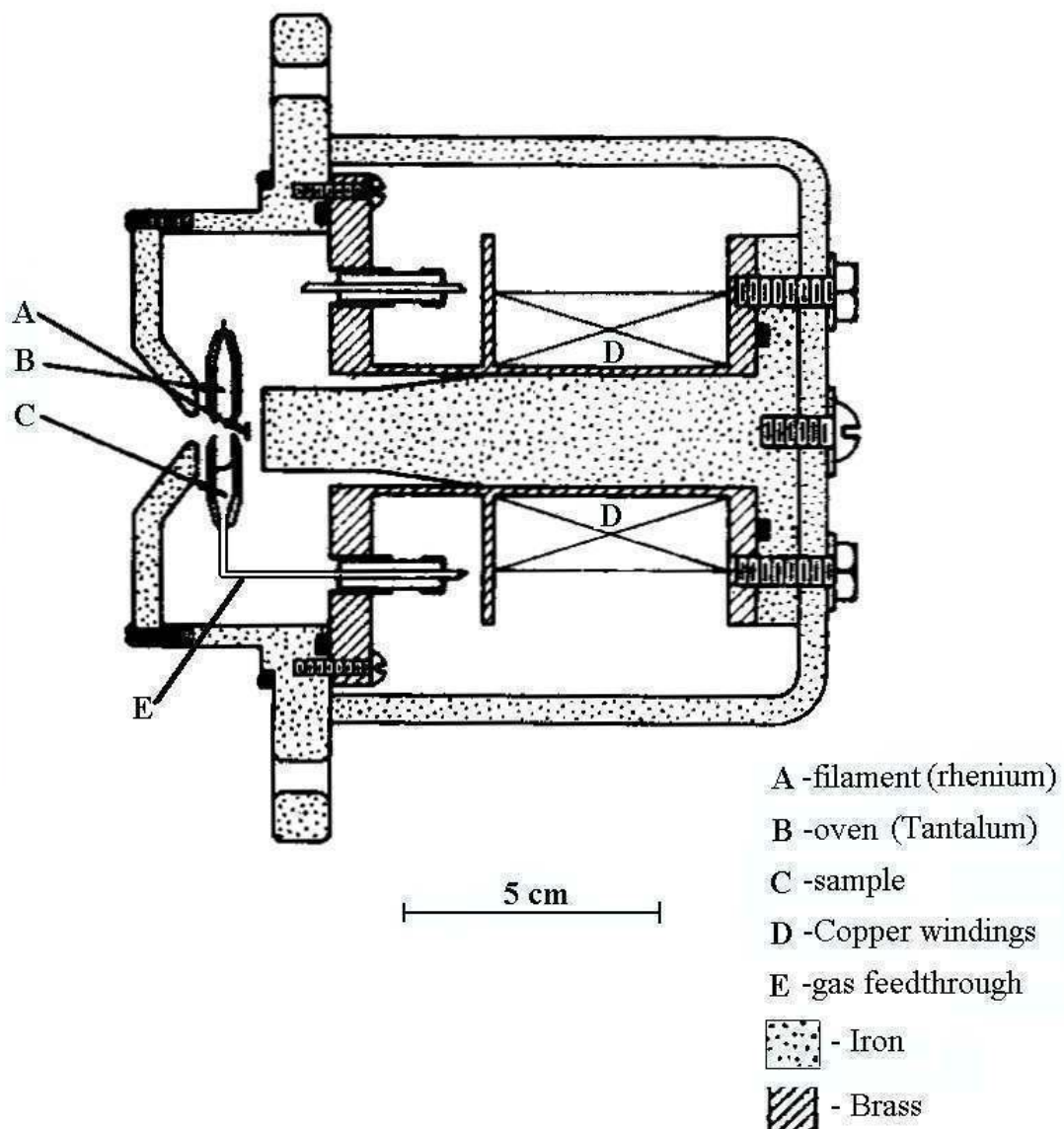


Fig.3-4 Modified Finkelstein Ion Source [Ba(1971)]

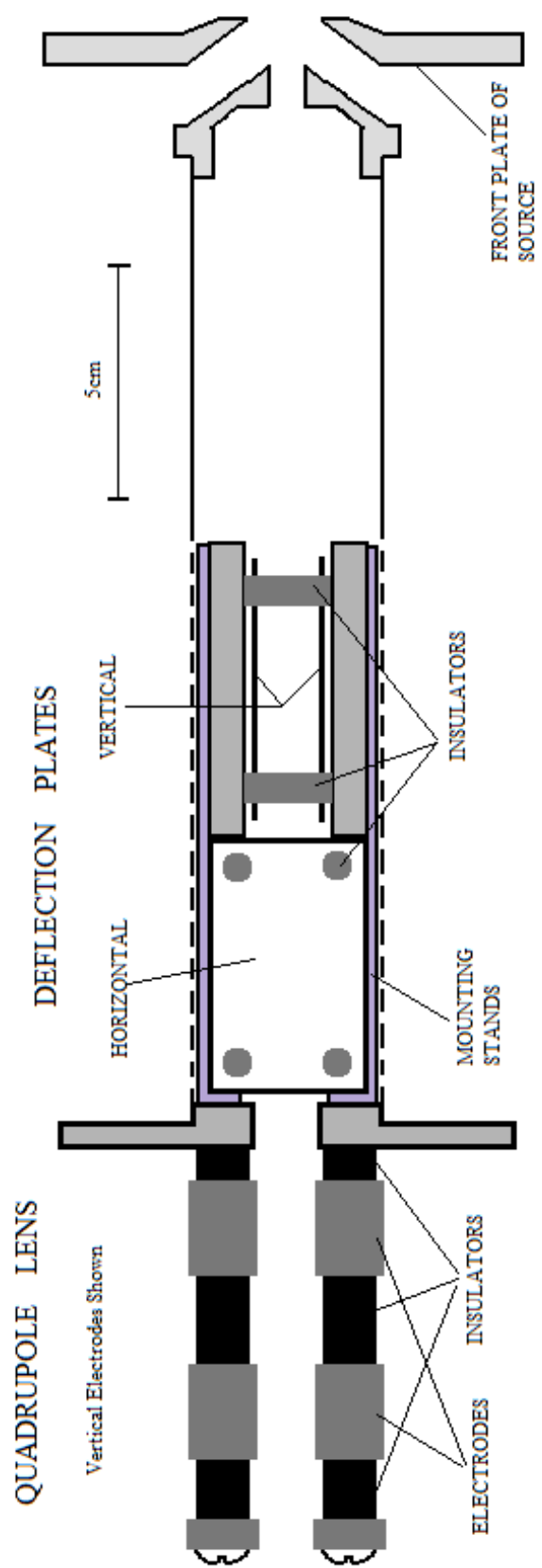


Fig. 3-5 Focusing and Steering Electrodes

3.2 Electrostatic Analyzer (ESA)

The ions pass through the α slit (which limits the angular spread of the beam) then enter the 1.0m radius ESA. The ESA consists of two gold plated cylindrical electrodes insulated with quartz blocks. The distance between each curved electrode plate is $2k = 2\text{cm}$ and is maintained at a consistent separation throughout by quartz spacers. Until around 1995, the potential source for the ESA plates was a very stable stack of Union Carbide 97.3V mercury reference batteries. These batteries exhibited a stability of a few parts in 10^{-9} . By the mid 1990's the unavailability of these batteries forced a change. Two Fluke 5440 precision voltage calibrators replaced the batteries. They provided a low noise and high stability potential required for accurate mass difference determinations.

The ESA is mounted on 3 steel ball bearings so that it and the source may be moved as one unit about a pivot located at the β slit. This point is located at the theoretical direction focus of the ESA and the object position for the magnetic analyzer. The β slit limits the range of energy of ions transmitted by the instrument. This slit has a width that is typically $\sim 3\text{mm}$, but can be increased or decreased.

The ESA is maintained at a pressure of around 5×10^{-8} Torr by an Edwards EXT250M Turbo molecular pump and a 50L/s ion pump that are connected midway on the ESA.

3.3 Magnetic Analyzer

The ions travel a distance of l_m' and then enter the magnetic analyzer. The magnet consists of 3 main C-shaped sections, each with 4 coil sections. Each coil consists of 60 turns of copper wire. The magnet is powered by a stable 200A Bruker (B-MN15/200) supply connected in parallel to each section and is cooled by a circulating water supply that runs through both the Bruker unit as well as the coils on each section. The main field or pole section has been accurately machined from Armco iron and has a 2.5cm gap for the ions to travel through. The ion gap is geometrically determined by precise stainless steel (type 304) blocks that were matched in size to within $\sim 5\mu\text{m}$.

The magnet also has two aluminum 'shimming' gaps that are $\sim 0.25\text{cm}$, and located 8cm above and below the main ion gap. The shimming gaps smooth out irregularities in the field created by different field line path lengths and slight differences in the magnetic yoke. It has been shown by Bishop [Bi(1969)] that 3 cm inside the physical boundary the field uniformity is on the order of $1/5000$ at $0.3\text{-}0.8\text{W/m}^2$.

In order to compensate for the focusing effect of the fringe field of the magnet, Nier suggested that this was equivalent to a uniform field that extended one gap width beyond the physical boundaries [Ne(1940)]. Kerwin showed that this was a good estimation of this effect [Ke(1963)].

A pressure of roughly 2×10^{-8} Torr is maintained in the magnetic sector and detector regions by another 50L/s ion pump located on the collector arm.

3.4 The Collector and Detector Region

After leaving the magnet the ions encounter the field generated by a Helmholtz coil pair that is driven by a sawtooth current. This field sweeps the ions across the collector slit at a determined frequency. Ions pass through the collector slit and are detected by a BURLE model no. 4830-G low noise electron multiplier channeltron. This channeltron has a dark current of 3 counts per 60 seconds when the multiplier is supplied with 3kV. We used a suitable 2.2kV supply for the channeltron. The signal is amplified and then fed to an oscilloscope for live display. The signal is also fed to a digital data acquisition (DDA) module which in turn sends a USB data packet to a digital signal averager (DSA) for live display and storing on a Linux based computer. The DSA stores information after every sweep which is later used for analysis.

As an aside it is important to keep the instrument at the lowest pressure possible. This is because the mean free path, λ , is inversely proportional to the pressure, i.e:

$$\lambda \text{ (in cm)} = (0.005)/P \quad (3-1)$$

where the pressure, P, is in Torr. The number of scattered particles N, from an ion beam of N_0 particles traversing a path length of X is:

$$N = N_0 e^{-\lambda/X} \quad (3-2)$$

So if the pressure increases, λ decreases, and the number of ions scattered will increase exponentially. With a pressure of around 3×10^{-8} Torr, the scattering value is very close to zero. Larger values of the pressure result in substantially more scattered ions which produces the tail end we see on ion peaks.

The entire instrument, including all the above components (except the computer devices), is mounted on a rigid table which, in turn, is supported by 8 bellows. The bellows are filled with Nitrogen gas in order to isolate the mass spectrometer from building vibrations.

3.5 Recent Modifications to Manitoba II

Prior to these studies, as noted in §3.2, Barillari [Ba(1999)] modified the voltage supply for the ESA to incorporate the two FLUKE reference supplies and the circuit which adds $\pm \Delta V/2$ to the output of the FLUKE supplies. Barillari, in the course of his work, also added a digital timing and Delta-V summing system (see Fig.3-6).

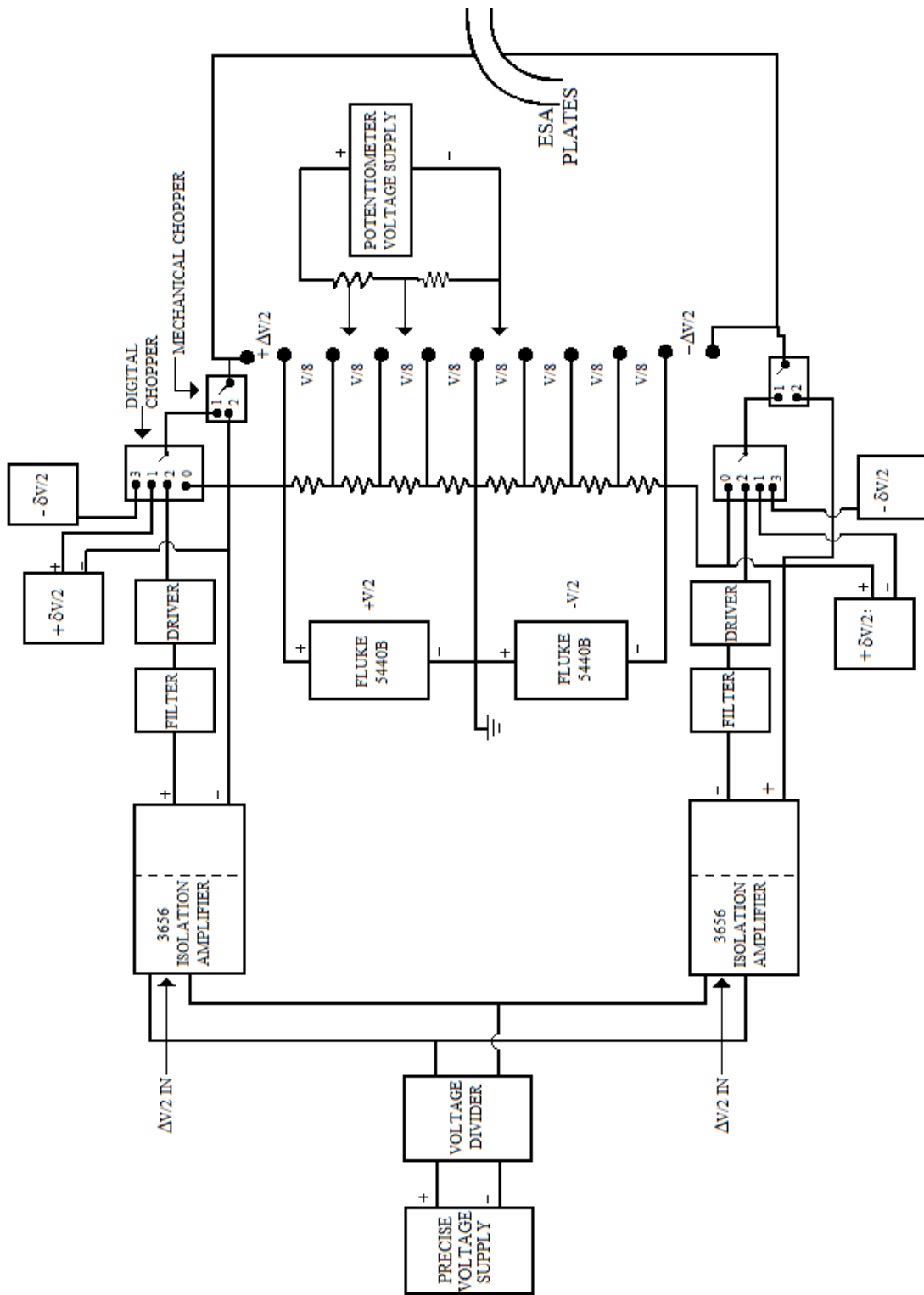


Fig.3-6 Potentials, Delta-V Summing System, and Potentiometer

It was decided in this study to incorporate a digital data acquisition and analysis system with the already-in-place digital apparatus from Barillari's work. Besides the minor upgrades associated with older circuits, the major additions are:

- A digital data acquisition module (DDA) and digital signal averager (DSA)
- A Real time digital analyzer for a desktop computer
- A new Master Trigger Control
- A new master sawtooth generator
- An improved link for switching the ion source accelerating potential, V_a

3.5.1 The DDA and DSA

For many years a Nicolet analog signal averager was used in the multiscaling mode to accumulate the counts from the channeltron. Following the failure of this apparatus, which was no longer repairable, it was decided in this work to build a digital signal averaging system that could be linked with a computer. This took advantage of the affordable, higher speed microchips available in today's market.

This was first proposed by Barillari, but in a slightly different form. The goal was to create a PCI board that would receive timing and channeltron signals, and then incorporate them into a computer signal averaging program. In this work an independent DDA module was built (Fig.3-7) which streamed data via USB to a Linux based PC. On the PC, the signal averaging (DSA) was done via a program (see Appendix B) called the *Analyzer*. Referring to the circuit A.1 in Appendix A, a Cypress CY7C64613-128NC 2nd generation full-speed USB microcontroller was used. This chip has a modified 8051 instruction set, which is popular among most embedded compilers. This makes it versatile for present and future computers. It also has an on-chip 'crystal' counter which allows the channeltron data, which is gate-delayed first, to be connected directly to the microcontroller; thus allowing for a synchronous operation. It acquires data from two timing signals and the channeltron signal. A block diagram showing the data capture process is given in Fig. 3-8. The computer program, via USB, receives the data only in full completed sweep packets. Every sweep packet is the data collected from all four quadrants. The PC program works like an oscilloscope and a data buffer in that it provides real time viewing, memory viewing (that is quadrant selective), a visual null matching option, and a data input screen (i.e. batteries, voltages, sweeps...etc.). The data can be saved in suitable file forms (*.dat for the AMDprime program or *.betsy for the *Analyzer* program) for later analysis. Refer to Appendix B for a visual step-by-step description of the analysis program.

3.5.2 New Trigger Master Control Board

Due to the aging electronics of the master trigger control and a problem of 'ringing', a new master trigger circuit was constructed to produce a clean OSC trigger and ZERO reset signal for data acquisition. This new circuit board performs the same

operations as the board it replaced, but has simplified them by providing only the signals we needed. Pictures can be seen in Fig.3-9, as well as a circuit diagram A.2 in appendix A.

3.5.3 New Sawtooth Generator

After making the ‘detector’ part of the machine fully digital, there was no need for the sawtooth generating oscilloscope. This oscilloscope was used as a master sawtooth generator in previous experiments on the Manitoba II. It generated a 100V sawtooth that triggered with every OSC trigger hit. This sawtooth waveform, was amplified by a bipolar operational amplifier in order to drive the Helmholtz coil pair that swept the ions across the collector slit (see §3.4).

Our new sawtooth generator (Fig.3-10) produced a 3V sawtooth and an inverted pulse for every OSC trigger pulse. This means that the previous bipolar signal converter board needed a change in gain resistors. The above circuits can be found, and labelled respectively, in appendix A.

3.5.4 Updated Source Voltage Switching

Referring to Fig. 3-2, the neon lamp that provided the timing for the source potentials (the high voltage and quadrupole lens) was replaced with an infrared phototransistor-emitter pair. This circuit ensures that the switching of the source potential, ΔV_a , is properly synchronized with the ΔV on the ESA.

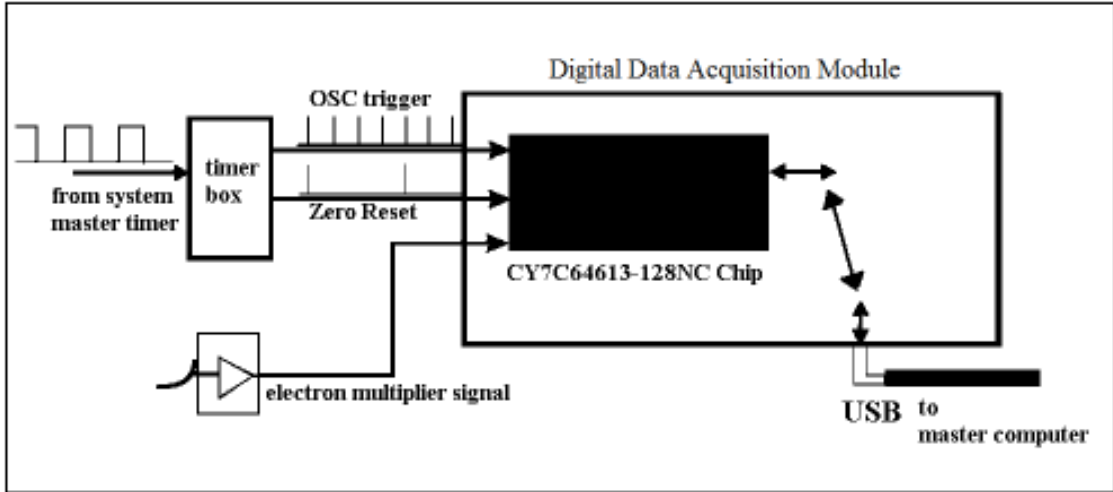


Fig.3-7a Block diagram of the new DDA set-up



Fig.3-7b The DDA Module (in workable beta form)

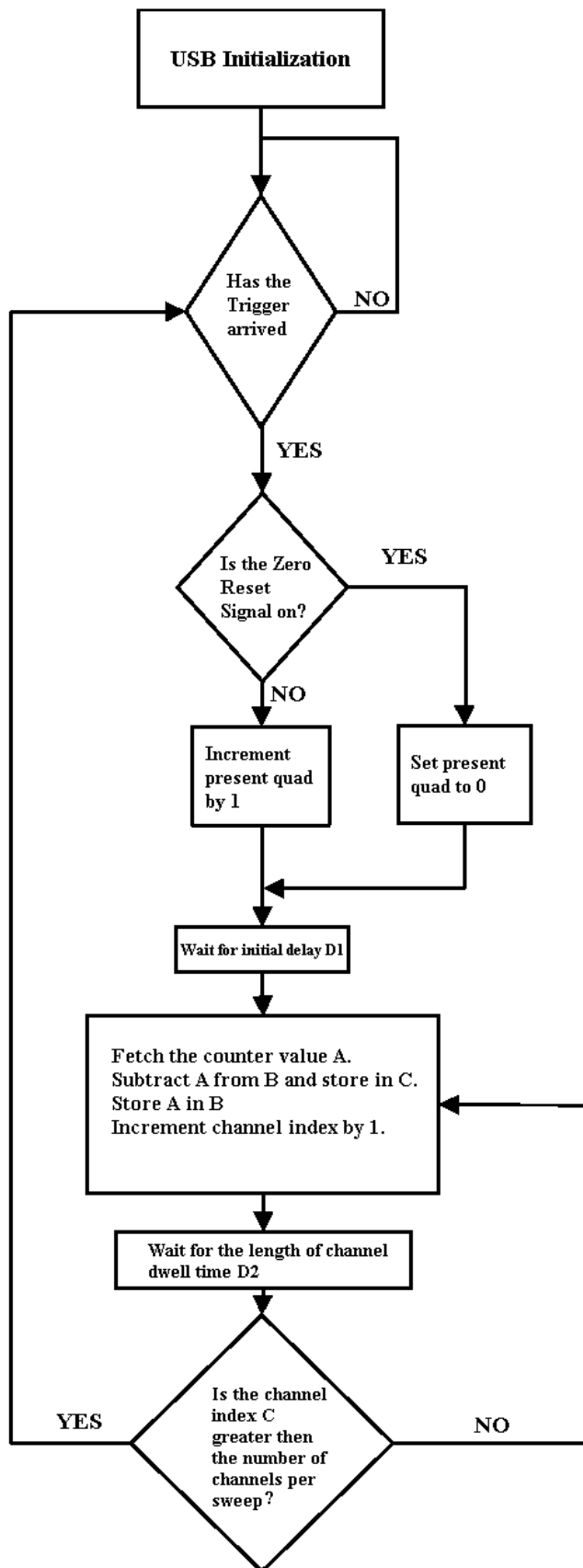
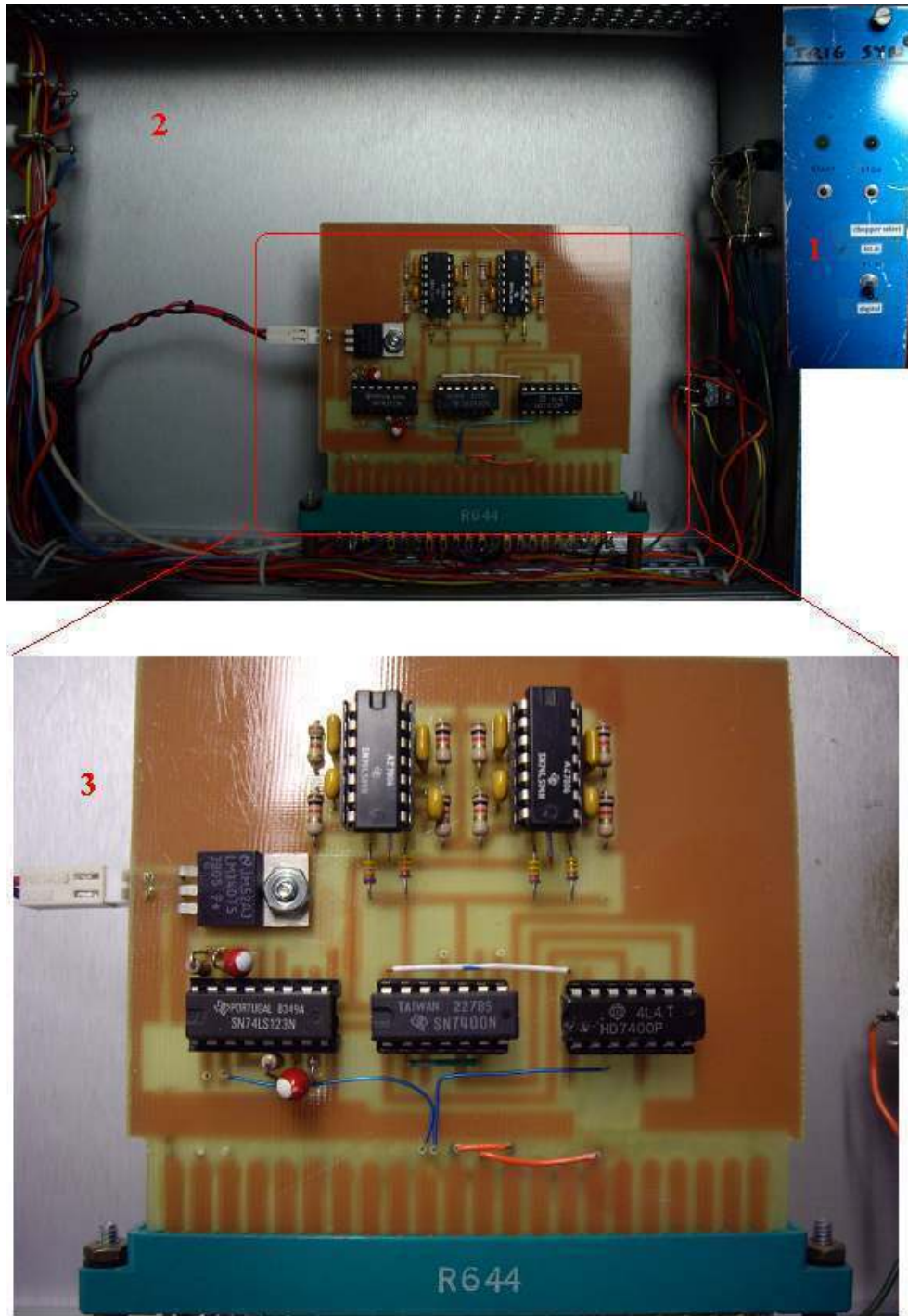


Fig.3-8 DDA data capture block-program



1-Front view of original trigger bin
 2-inside side view of trigger bin
 3-new trigger control circuit

Fig.3-9 New Trigger Master Control



Fig.3-10 New Sawtooth Generator



Fig.3-11 The Mantioba II

Chapter 4

Experimental Procedures

4.1 Start-Up Procedures

The 'start-up' of the instrument proceeded if the ion source pressure was satisfactory ($\sim 2 \times 10^{-6}$ Torr). First, the bellows supporting the table and isolating the instrument from building vibrations were inflated. The source potentials were then turned on, in the listed order, to the approximate values:

- | | |
|----------------------------------|------------------------|
| 1) Electron accelerating voltage | ~ 120-150V |
| 2) Repeller voltage | ~ 400V |
| 3) Magnetic Current Supply | ~ 4-5A |
| 4) Filament Current Supply | ~ 8-10A |
| 5) Oven Heater Current | ~ up to a max of 17.5A |
| 6) High Accelerating Potential | ~19.7kV |

The filament was heated slowly at the start, beginning at ~ 5 A then up to ~ 10 A, and was adjusted so that the emission current reached a steady 6-10mA. At this point the high voltage was turned on. Once a steady emission current was attained, the heating current of the oven was increased in small increments so that the sample started to vapourize. The source oven was heated by two Re ribbons connected in parallel, one for each end of the oven to insure uniform heating. For the BaCl_2 sample, the oven was heated up to $\sim 15 - 18$ A before high ion intensity or plasmas were formed, i.e. 7.5 - 9A in each ribbon.

The quadrupole and steering plate voltages, Helmholtz coil supply, the ESA voltage supply, and the magnetic analyzer current supply were then turned on. The ESA plates were set to ± 388.8 V each, while the magnet current varied depending on the isotopic species being studied (usually ^{35}Cl was around 1440 bruker units in the BORIS magnetic controller program-see [Ba(1999)]). With both object and image slits opened, the source isolation valve was then opened. A 2.2kV supply powered the electron multiplier. The ion beam was steered by the horizontal and vertical deflection plates (fig.3-5) until an ion peak was swept across the live display (of either the oscilloscope or the computer).

Experimentally, it's necessary to make adjustments to the instrument to achieve a double focus. Direction focusing was achieved by carefully balancing two geometrical adjustments. In most cases this involved adjusting both l_e and moving the ESA about its pivot point. As noted earlier, the β slit that limits the range of energy of the transmitted ions is located at the pivot point (the theoretical direction focus) of the ESA. If the ESA is

moved to change the angle of entry of the ions into the magnetic analyzer, the direction focus for the magnet should be where the peaks change direction on the live display while swinging the ESA about its pivot point. If the direction focus occurs at this angle, the direction focus of the ESA is located at the β slit, and the direction focus of the combined fields is at the collector.

At the direction focus, the beam rises and falls, rather than moves from side to side on the live display, when the horizontal deflection voltage is varied. When the beam is direction focused substantial improvement in ion peak resolution is observed.

Velocity focusing is tested by adding a 10-20V square wave to the high voltage so that ions on alternate sweeps have an energy increased by that amount. If alternate sweeps on the oscilloscope are displaced, the ion beam having higher energy can be compared to the normal ion beam. If the two peaks are aligned vertically then the ion beam is velocity focused. If not, the detector slit is physically moved transversely to the beam, while the field is adjusted to keep the peak on the screen. This adjustment effectively changes r_m by a small amount, as required by equation (2-15). Both the velocity and direction focusing slightly affect one another. Once a velocity focus is obtained, a slight adjustment to the direction focus is made and vice versa. When this 'first-order' adjustment is completed, to the discretion of the experimenter, 'second order' focusing is assured by the instrument's geometry [Ba(1964)].

4.2 Peak Matching

With the principal and image slits adjusted to allow the best resolution possible, the peaks or mass differences may be measured. The measurement technique is based on Bleakney's theorem (see §2.2).

Using a master timing signal we switch, on alternate sweeps, the accelerating potential, the deflecting plates, the quadrupoles, and the electrostatic analyzer simultaneously as required by Bleakney's theorem. For closely separated peaks, the peak position is not sensitive to the quadrupole, high voltage, and deflection plate potentials. The accuracy need only be about 1%. In contrast, the peak position is extremely sensitive to the voltages across the ESA. These are measured precisely, to a part in 10^{-9} V (i.e. $\sim \pm 0.8\mu\text{V}$), by a custom built null potentiometer voltage divider using Julie Research precision resistors [Bi(1963)].

Fig. 3-6 shows a diagram of the ΔV summing system for the ESA plates. The application of a $\pm\Delta V/2$ and $\pm\delta V/2$ along with the FLUKE potentials are supplied to the ESA plates in a timed sequence set by a master timing signal. With this apparatus, one can perform either a visual match or a computer match.

Fig. 4-1 shows in detail the system of timing that switches the voltages as required for peak matching. Timing signals are produced by a digital chopper discussed

in detail by Barillari [Ba(1999)]. The chopper creates A and B signals which, in turn, produce timing signals for the high voltage, the Helmholtz supply, the DDA, and the Delta-V summing system.

Since the speed of digital data acquisition has increased dramatically over the last 10 years, the use of visually matching a pair of peaks has been used only as a preliminary step towards computer matching. Visual null matching is the process of using only two quadrants, zero and ΔV , then superimposing the two split signals by inverting the acquired memory of one against the acquired memory of the other. The two signals have gain adjustments to ensure that the peaks have close to identical amplitudes. If, using the DDA and the *Analyzer* program (refer to appendix B), one can simply input the peak ratio and the program adjusts the gain appropriately. If the resultant image is an s-shape, then the two peaks are not matched. At this point the ΔV is adjusted carefully by the operator until they are matched. When they are matched, only an oval pattern of noise is seen (refer to fig. 4-2). Once the experimenter is certain of a good voltage match, the ΔV for the setting is measured. The use of the visual matching in this work was limited to calibration doublets where high precision was not required.

4.3 Computer Matching

Referring to fig.4-1 we see the trigger signals that control the switching to one of the four voltage quadrants: ΔV , the voltage being applied to the ESA plates in order to match two peaks on the display, $\pm\delta V$, the voltage splits applied to the ESA plates for data analysis, usually about 10,000 to 100,000 times smaller than ΔV (which correspond to a peak displacement of about 1/10 of a peak width), and the zero quadrant, where no voltage is applied to either plate other than $\pm 388.8V$. The reset signal tells the delta-V system to revert back to the ΔV quadrant. It switches through the four quadrants then cycles again. The trigger signal also creates the sawtooth for the Helmholtz sweeping coils. It should be noted that the sweep occurs slightly after the voltage has switched and ends before the next voltage starts and allows for a settling time for the switched voltages. This is to avoid any counts that are associated with any other quadrant sweeps. The trigger and reset signals are also important to the DDA module (see §3.5.1).

Computer matching differs from visual matching in two ways: first, there are four (see fig.4-1 & 4-3), rather than two, quadrants of data acquired, and second, the data is stored in the computer for later analysis using the AMDprime (ver.6.5) program. Computer matching reduces sensitivity to variations in peak intensity and provides higher precision with off-line analysis. The extra two quadrants add and subtract a small δV to the plates. These 'splits' are small applied voltages that create an upper and lower limit to the larger ΔV . Thus when these values are used in a centroid matching algorithm, the best value between $\Delta V + \delta V$ and $\Delta V - \delta V$ for a match is calculated.

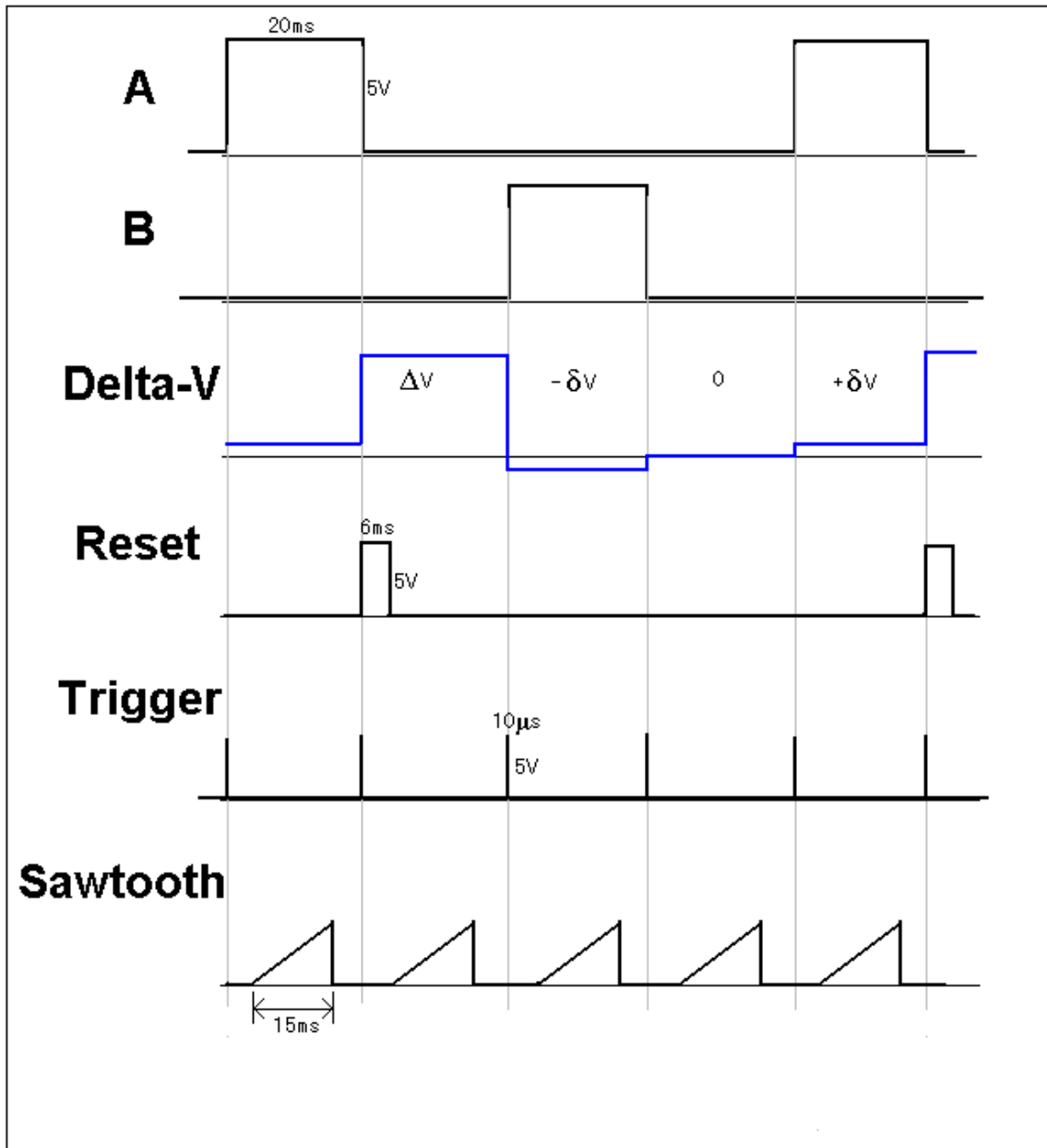


Fig.4-1 Master Timing Signals of the Manitoba II

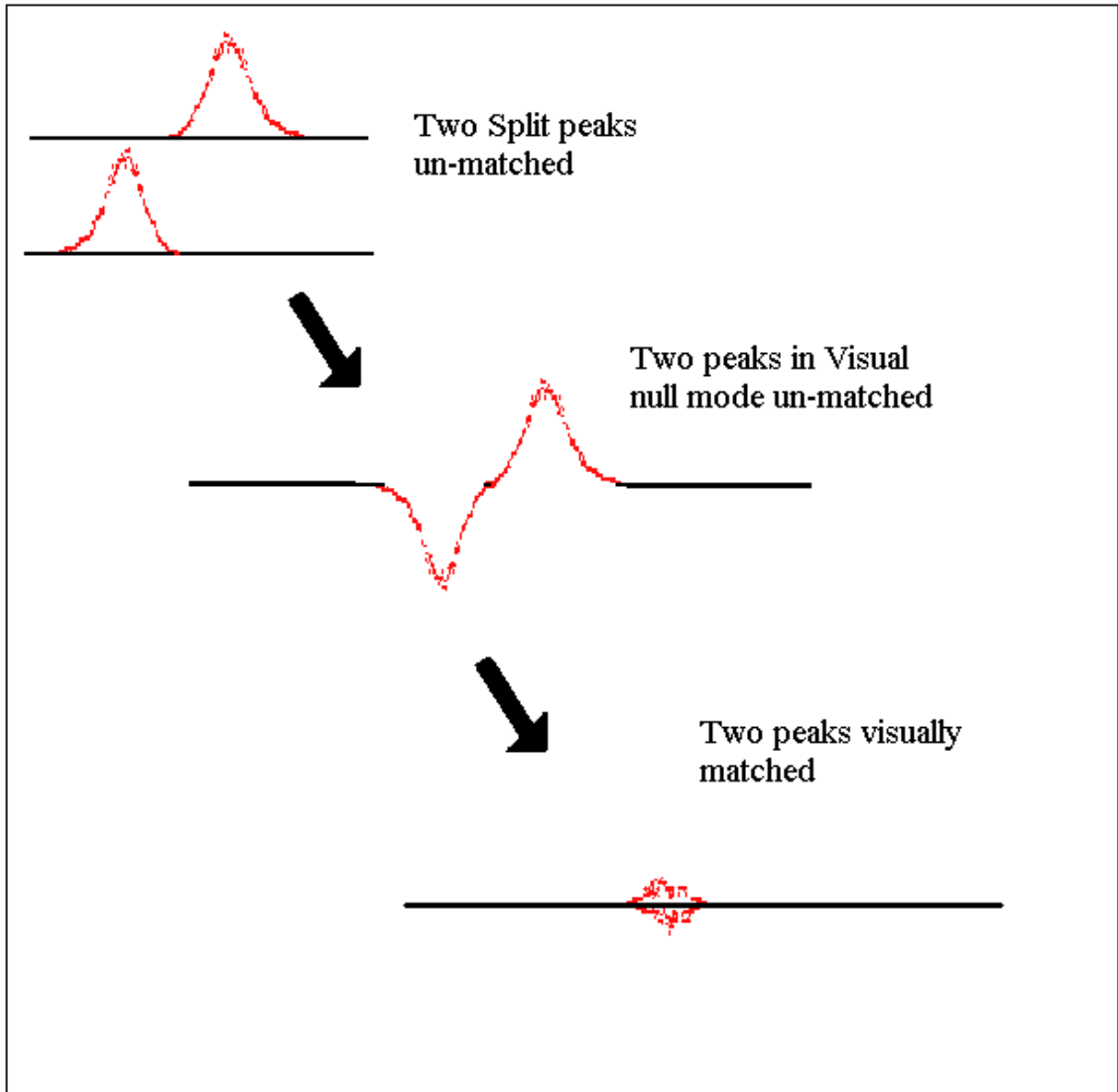


Fig.4-2 Visual matching

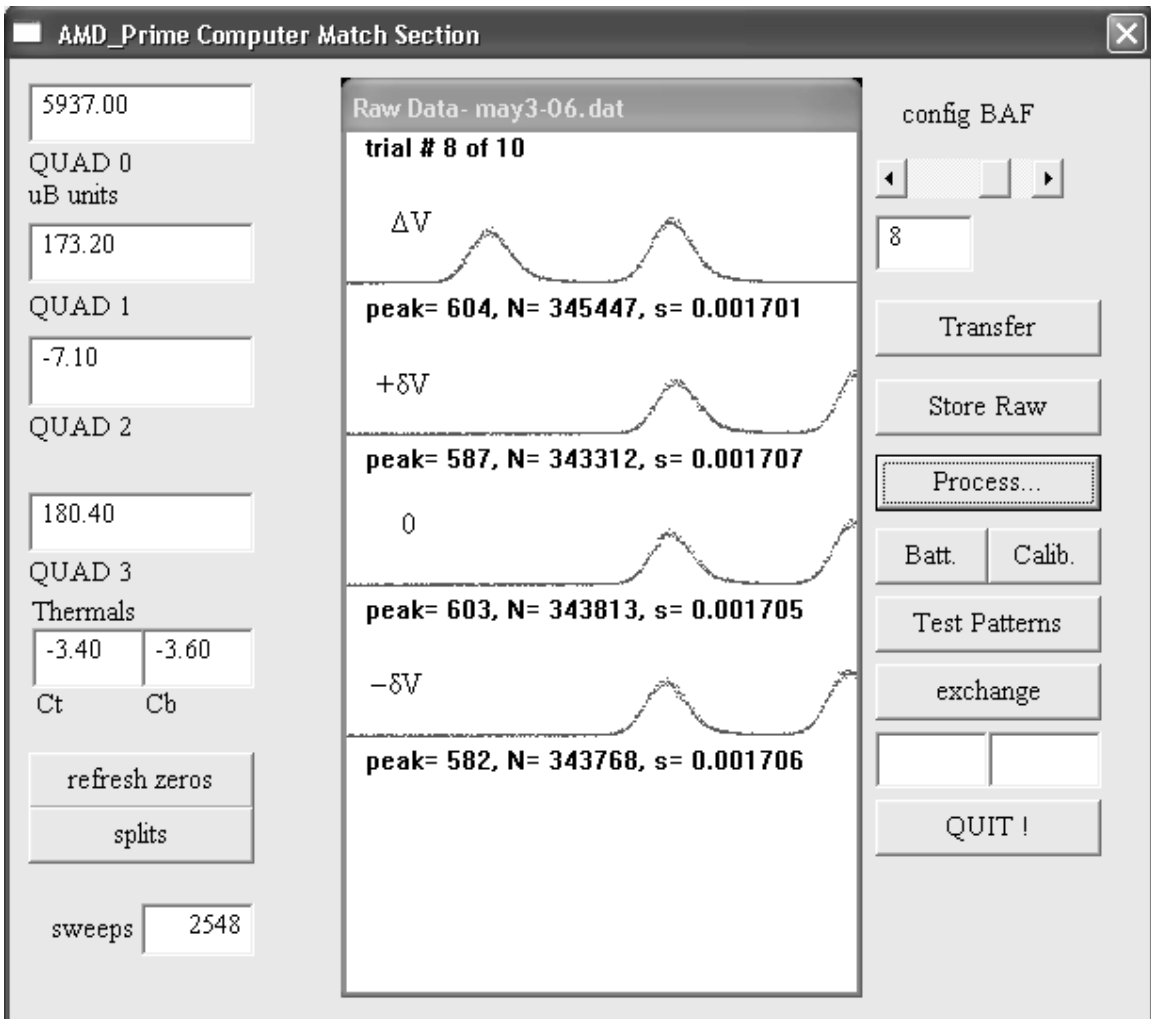


Fig.4-3 A Typical BAF Computer Match Configuration in AMDprime

A single digital run consists of eight configurations which vary voltage and sweep direction. This is done to eliminate systematic errors. The eight configurations are denoted by a three letter acronym. The first letter determines the sequence of the splits, whether they are normal (N), as in Fig. 4-1, or backwards (B), such that the $+\delta V$ comes before the $-\delta V$. The second letter indicates whether ΔV is added (A) or subtracted (S). The last letter describes whether the sweep is forward (F) or reversed (R): For example, NAR refers to a normal arrangement of the splits, the adding of ΔV , and a reverse sweep. The eight configurations in a single computer match run are: NAF, BAF, BAR, NAR, NSF, BSF, BSR, and NSR.

4.4 Digital Acquisition

The output of the channeltron data is buffered and stored in the DDA. The data for one sweep is accumulated, where that sweep count is then sent via USB to the *Analyzer* on the computer. One sweep counts as the data acquired from all four quadrants in one cycle. The data is then viewed via the memory display in the program (refer to appendix B).

The measured voltages are entered in the ‘*Volt*’ field for each matching configuration. The batteries are measured using a null potentiometer which is an 8 component resistor chain that provides an accurate measurement of the ESA potential (see [Bi(1963)]). After each configuration measurement (NAF, NAR ...) the splits were measured. The ΔV was measured at the beginning, middle and end of all eight configurations, and the zero quadrant was measured after every two measurements. The zero quadrant measurement usually produced a slight non-zero potential due to thermal Emf’s and contact potentials in the potentiometer. The thermals were usually on the order of 0-38 μV .

All potentials entered into the *Analyzer* program are in “micro-Bishop (μBp) units”. The ‘Bp’ unit was introduced by Bishop [Bi(1963)] as a lab unit of convenience that originated with the design of the potential divider and is:

$$1Bp \approx 3.782V \quad (4-1)$$

The file in the *Analyzer* program is then saved to a *.dat file and is now ready to be transferred to AMDprime for analysis.

4.5 Data Analysis

A step-by-step user guide of the most recent version of AMDprime can be found in Barillari’s work [Ba(1999)].

After centroid fitting mass peaks in AMDprime the program calculated a mass difference, δM , and an error, σ , for each configuration. For all eight configurations that make up one run, a weighted mean of the δM 's was calculated by:

$$\Delta M_{\text{wgt}} = \frac{\sum_i \frac{\delta M_i}{\sigma_i^2}}{\sum_i \frac{1}{\sigma_i^2}} \quad (4-2)$$

Two errors are calculated along with the mean [Bi(1932)]. The internal error, σ_{int} , is the estimated error in the mean due to the size of each σ_i :

$$\sigma_{\text{int}}^2 = \frac{1}{\sum_i \frac{1}{\sigma_i^2}} \quad (4-3)$$

The external error, σ_{ext} , expresses the size of the scatter of each δM about the mean ΔM :

$$\sigma_{\text{ext}}^2 = \left(\frac{1}{N-1} \right) \frac{\sum_i \frac{(\Delta M - \delta M_i)^2}{\sigma_i^2}}{\sum_i \frac{1}{\sigma_i^2}} \quad (4-4)$$

where N is the number of configurations used; in all cases it was 8. We will use the same approach as Meredith [Me(1971)], where the larger of these two errors is then used to calculate the final weighted mean and error for the 5 runs of each doublet.

The number of runs for a match depended on the peak difference being sought. If it were a narrow doublet or if there were an odd ratio in peak intensities, more runs would be required. For this experiment 5 runs were made for each doublet in order to minimize the error to within acceptable values. Errors on the order of $0.50\mu\text{u}$ were typical.

The 'u' is an atomic mass unit [Au(2003)] where:

$$1\text{u} = \left(\frac{1}{12} \right) M(^{12}\text{C}) \quad (4-5)$$

where the mass, M , is an isolated ^{12}C atom in its atomic and nuclear ground state. In terms of SI units 'u' is:

$$1\text{u} = 1\,660\,538.73 \pm 0.13 \times 10^{-33} \text{ kg} = \frac{1\text{g}}{N_A} \quad (4-6)$$

or,

$$1 u = 931\,494.013 \pm 0.037 \text{ keV} \quad (4.7)$$

After the least squares analysis is done, a consistency check of the data, using a reduced chi-squared evaluation, is performed. The reduced chi-squared formula is thus:

$$\chi_{n-1}^2 = \left(\frac{1}{n-1} \right) \sum_i \frac{(\Delta M - \delta M_i)^2}{\sigma_i^2} \quad (4.8)$$

where (n-1) are the degrees of freedom. The reduced chi-squared formula should be as near to one as possible for a strong fit to the data.

Chapter 5

Results

5.1 Motivation for the Measurement of $^{136}\text{Ba} - ^{136}\text{Xe}$

In this thesis, measurements of atomic mass differences amongst some Ba and Cd isotopes and a measurement of $^{136}\text{Xe} - ^{136}\text{Ba}$ are reported. The latter is of special interest because it is presently a good candidate for neutrinoless double beta-decay. If such a neutrinoless decay is observed, it would provide strong evidence for a massive neutrino having a non-zero rest mass.

In neutrinoless double beta decay, all of the reaction energy is given to the beta particles. In an energy spectrum, a sharp peak would be located at the Q-value of the decay. In order to set an upper limit for the lifetime of this decay, the energy at which this peak occurs must be known. By Einstein's mass-energy relation [Ei(1905)], the Q-value for the decay is obtained by measuring the mass difference $^{136}\text{Xe} - ^{136}\text{Ba}$.

5.2 Experimental Details

As has been the standard operating procedure, calibration doublets were determined [So(1973)]. Wide calibration doublets (i.e. where ΔM is 1 or 2 mass units) are used to determine the correction that is required to take into account the presence of surface charges on the ESA. The presence of such charges produce an electric field seen by the ions that is slightly different from the applied electric field associated with the applied (and measured) potential. All calibration measurements used a ΔM of 1u, either heavier or lighter, whichever was more convenient. Most systematic corrections, adjusted by data input on the AMDprime program, were on average around 220ppm, but sometimes were as large as 380ppm.

The cadmium doublet, $^{116}\text{Cd}^{35}\text{Cl} - ^{114}\text{Cd}^{37}\text{Cl}$, was measured first to confirm that the new DDA and DSA were working correctly with the rest of the instrument. In finding that the new additions worked correctly, the measurement also provided a more precise value for the doublet and a reduced associated uncertainty compared to the previous value by Meredith [(Me(1973))].

The next two doublets measured were $^{137}\text{Ba}^{35}\text{Cl} - ^{135}\text{Ba}^{37}\text{Cl}$ and $^{138}\text{Ba}^{35}\text{Cl} - ^{136}\text{Ba}^{37}\text{Cl}$; masses 172 and 173 respectively. A BaCl_2 sample was used in the tantalum oven and the BaCl spectrum was analyzed. These doublets provided experience in the operation of the ion source with the BaCl_2 sample.

Finally a measurement of $^{136}\text{Xe} - ^{136}\text{Ba}$ was made. A Xe gas cylinder was pressure limited and then connected to our source by polyflo tubing and a needle valve. The needle valve limited the volume of gas entering the oven.

5.3 Experimental Results

There were a total of 4 doublets measured during the course of this work. They are shown in the tables below:

TABLE 5-1 Raw Data

Doublet	Weighted Means (μu)	σ_{int}	σ_{ext}	Standard Means (μu)	Sys. Corr. (ppm)	χ^2_{n-1}
$^{116}\text{Cd}^{35}\text{Cl} - ^{114}\text{Cd}^{37}\text{Cl}$	4347.481	0.669	1.177	4346.160	230	1.08
	4347.814	0.788	1.733	4346.205	230	1.23
	4347.399	0.120	0.883	4347.609	172	1.15
	4347.520	0.167	1.490	4346.831	256	1.05
	4347.430	0.625	0.664	4347.250	172	1.11
$^{137}\text{Ba}^{35}\text{Cl} - ^{135}\text{Ba}^{37}\text{Cl}$	3090.751	1.111	1.339	3090.978	123	1.45
	3089.213	1.124	1.297	3089.623	123	1.33
	3088.790	1.057	1.221	3088.870	254	1.33
	3087.618	1.373	1.386	3087.834	254	1.02
	3088.891	1.381	1.435	3088.796	261	1.08
$^{138}\text{Ba}^{35}\text{Cl} - ^{136}\text{Ba}^{37}\text{Cl}$	3620.670	1.286	1.336	3620.930	382	1.08
	3620.902	1.258	1.267	3619.887	382	1.02
	3621.518	0.778	0.887	3621.486	350	1.30
	3620.968	0.870	1.617	3621.118	351	1.65
	3621.048	0.846	1.337	3620.080	351	1.30
$^{136}\text{Xe} - ^{136}\text{Ba}$	2639.559	1.139	1.359	2639.816	154	1.42
	2640.247	1.286	1.334	2640.461	154	1.08
	2638.690	0.968	1.281	2640.889	168	1.27
	2639.527	1.274	1.352	2640.764	168	1.13
	2639.817	1.160	1.370	2639.688	179	1.39

The systematic corrections from the wide calibration doublets are shown as well as the reduced chi-squared for each run. The data showed good agreement between weighted and standard means and had reasonable reduced chi-squared values. The weighted mean and error of each doublet are shown in table 5-2.

TABLE 5-2 Final Results

Code	Doublet	Value (μ u)	Uncertainty (μ u)	other author values	References
A	$^{116}\text{Cd}^{35}\text{Cl} - ^{114}\text{Cd}^{37}\text{Cl}$	4347.46	± 0.44	4348.7 ± 1.2	Meredith <i>et al.</i> [Me(1973)]
				4347.4 ± 2.2	Audi <i>et al.</i> [Au(2003)] adjusted value
B	$^{137}\text{Ba}^{35}\text{Cl} - ^{135}\text{Ba}^{37}\text{Cl}$	3089.07	± 0.60	3088.89 ± 0.10	Audi <i>et al.</i> [Au(2003)] calculated
C	$^{138}\text{Ba}^{35}\text{Cl} - ^{136}\text{Ba}^{37}\text{Cl}$	3621.13	± 0.54	3621.39 ± 0.10	Audi <i>et al.</i> [Au(2003)] calculated
D	$^{136}\text{Xe} - ^{136}\text{Ba}$	2639.55	± 0.60	See table 4-3	

5.3.1 Discussion of Results

The measured Cd doublet provided a more than satisfactory confirmation of the instrument's new digital data acquisition implementation as described in §3.5.1. It agrees with Meredith's value, which was done using the same instrument 35 years ago, but with improved precision. This improvement in precision has been achieved by the implementation of the present computer matching technique and analysis. It is also seen that the 'best-value', derived from the least squares evaluation by Audi *et al.* [Au(2003)], of all the data in this region, is in excellent agreement with the new measurement. Overall this measurement provided excellent confidence for further doublet determinations using the digital data acquisition additions.

The Ba doublet values agree very well with calculated values from the Atomic Mass Evaluations (AME) table [Au(2003)]. The Ba mass differences of the AME (Audi *et al.*) reflect the extremely precise and reliable (n, γ) Q-values that are used for input. This means that, again, the Ba doublets provide another stringent test on the reliability of the new $^{136}\text{Xe} - ^{136}\text{Ba}$ measurement.

The $^{136}\text{Xe} - ^{136}\text{Ba}$ measurement is compared to four other values shown in Table 4-2. The $Q_{\beta\beta}$ -value determined in this work should be taken in high confidence due to the excellent agreement of the Ba and Cd doublets.

TABLE 5-3 Double Beta-Decay Energies of ^{136}Xe

Doublet	$Q_{\beta\beta}$ (keV)				
D	This Work	Audi <i>et al.</i> Adjusted value [Au(2003)]	Monte Carlo Computation [Av(2005)]	ISOLTRAP ^{136}Xe measurement [He(2006)]	FSU Penning Trap ^{136}Xe measurement [Re(2007)]
$^{136}\text{Xe} - ^{136}\text{Ba}$	2458.72(56)	2462(7)	2479(79)	2462.7(4.3)	2457.83(37)

The value measured in this work agrees very well with the Audi *et al.* value and falls within the large uncertainty of the Monte Carlo result.

Another measurement of ^{136}Xe was done in 2006 using the ISOLTRAP [He(2006)]. The value for the mass of ^{136}Xe was determined to be $135\,907\,219.7 \pm 4.2\mu\text{u}$. Using this value, the ^{136}Ba value from the Atomic Mass Evaluations [Au(2003)] and Eq.4-7 gives another value for comparison. Our value is in agreement within uncertainty.

A recent measurement of ^{136}Xe , determined by the Florida State University Penning trap (to a part in 10^{-10}) [Re(2007)], was used along with the ^{136}Ba value from the 2003 AME Table [Au(2003)] to yield a low uncertainty $Q_{\beta\beta}$ -value. The consistency of their mass measurements for 3 different charge-states (3+, 4+, and 5+) of ^{136}Xe is convincing evidence that their result is the most accurate to date. Our value is very close to the FSU value. The sum for the probable errors on the difference of the two is 0.67keV. However, this depends on there being no systematic bias to the ^{136}Ba mass from the mass table. For this reason, a Penning trap measurement of the mass of ^{136}Ba should be strongly encouraged.

Overall the Q-value found in this work agrees with all the recently *calculated* ^{136}Xe $Q_{\beta\beta}$ -values. It is also interesting to note that our value falls in between the ISOLTRAP value and the FSU value. It is important, and should be noted, that this experiment is the first to directly determine the mass difference between ^{136}Xe - ^{136}Ba , and in combination with the FSU ^{136}Xe measurement will provide important information for future $\beta\beta 2\nu$ and $\beta\beta 0\nu$ determination experiments involving ^{136}Xe .

5.3.1 Implication of Results

The best and most recent decay-energy spectrum of ^{136}Xe to date is from the DAMA group located at the Gran Sasso Laboratory [Be(2002, 2003, 2006)]. Using a 6.5kg pure liquid Xe scintillator (Kr-free enriched in ^{136}Xe), an energy spectrum for ^{136}Xe

was produced from 8823.54 hours of data. It is shown in fig.5-1 and magnified to the area of interest in fig.5-2. This works $Q_{\beta\beta}$ -value is shown in fig. 5-2.

The energy bins of the DAMA experiment are 50keV and provide insufficient information to permit a maximum likelihood analysis using the $Q_{\beta\beta}$ from this work. It should be noted that in fig.5-2 there is a definite probability that an energy peak does exist very close to the 2459keV area, but the 2450-2499keV bin only differs by 2-8 counts (at the most) with the background. Better resolution is clearly required.

It is clear that the value attained in this work will be useful in future and present Xe experiments. Experiments already in progress, like EXO, will provide better energy resolution with lower background counts and a much improved energy spectrum for ^{136}Xe around the 2400 – 2500 keV range. This will help determine the nature of this double beta-decay.

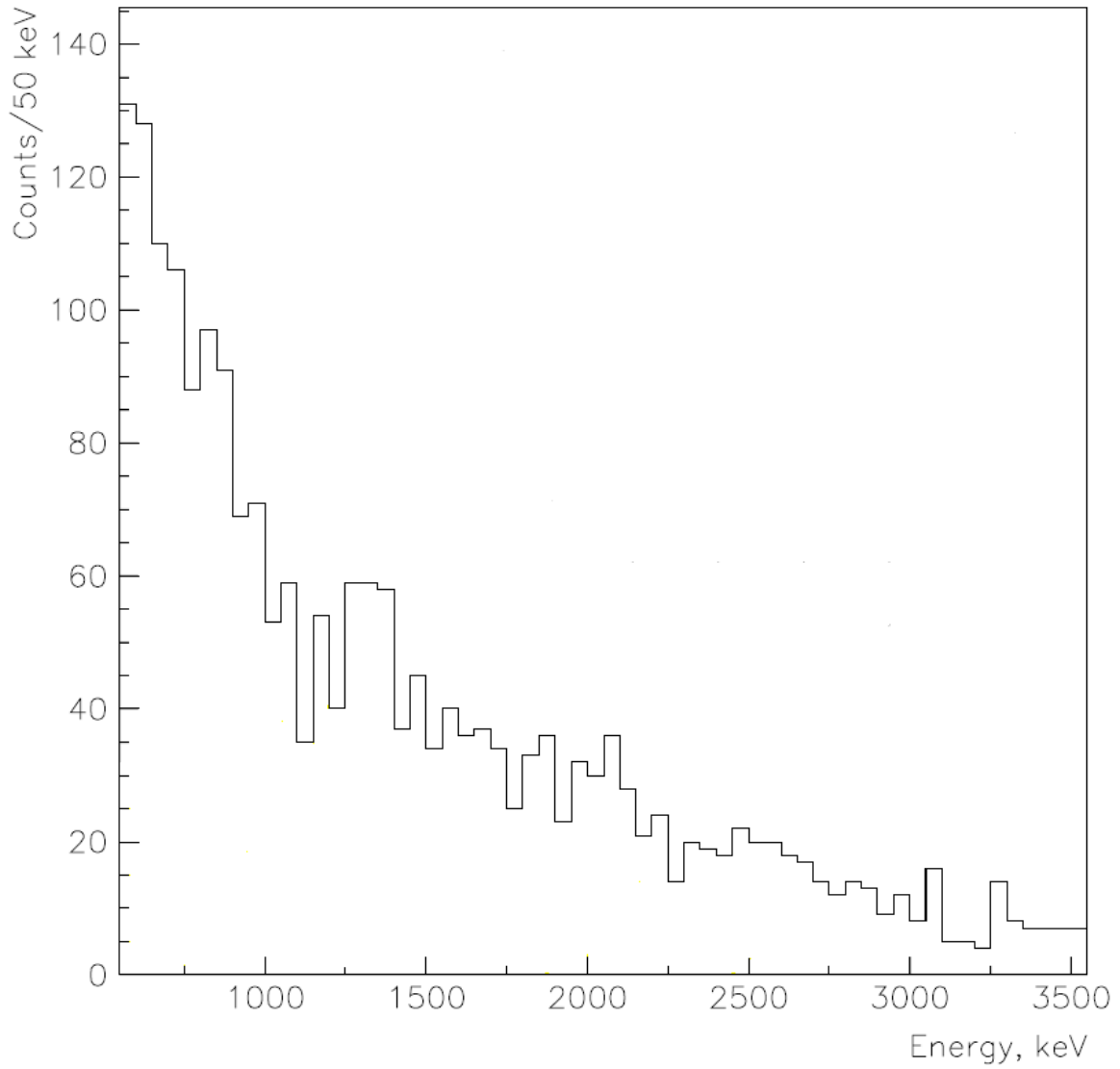


Fig.5-1 ^{136}Xe Energy Spectrum after 8823.54 hours of data taking from the \sim 6.5kg pure LXe detector of the DAMA experiment [Be(2003)]

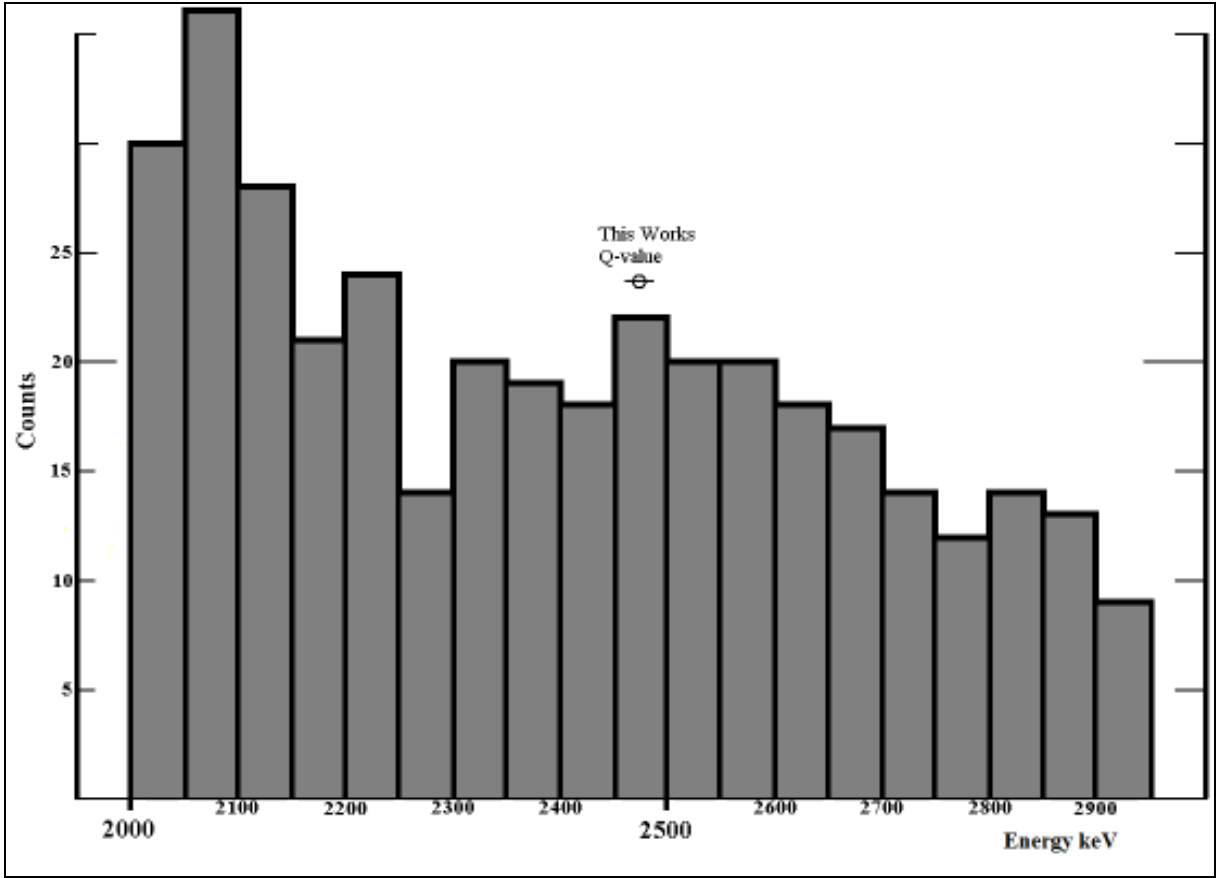


Fig.5-2 ^{136}Xe Energy Spectrum after 8823.54 hours of data taking from the $\sim 6.5\text{kg}$ pure LXe detector of the DAMA experiment magnified to the area of interest.

References:

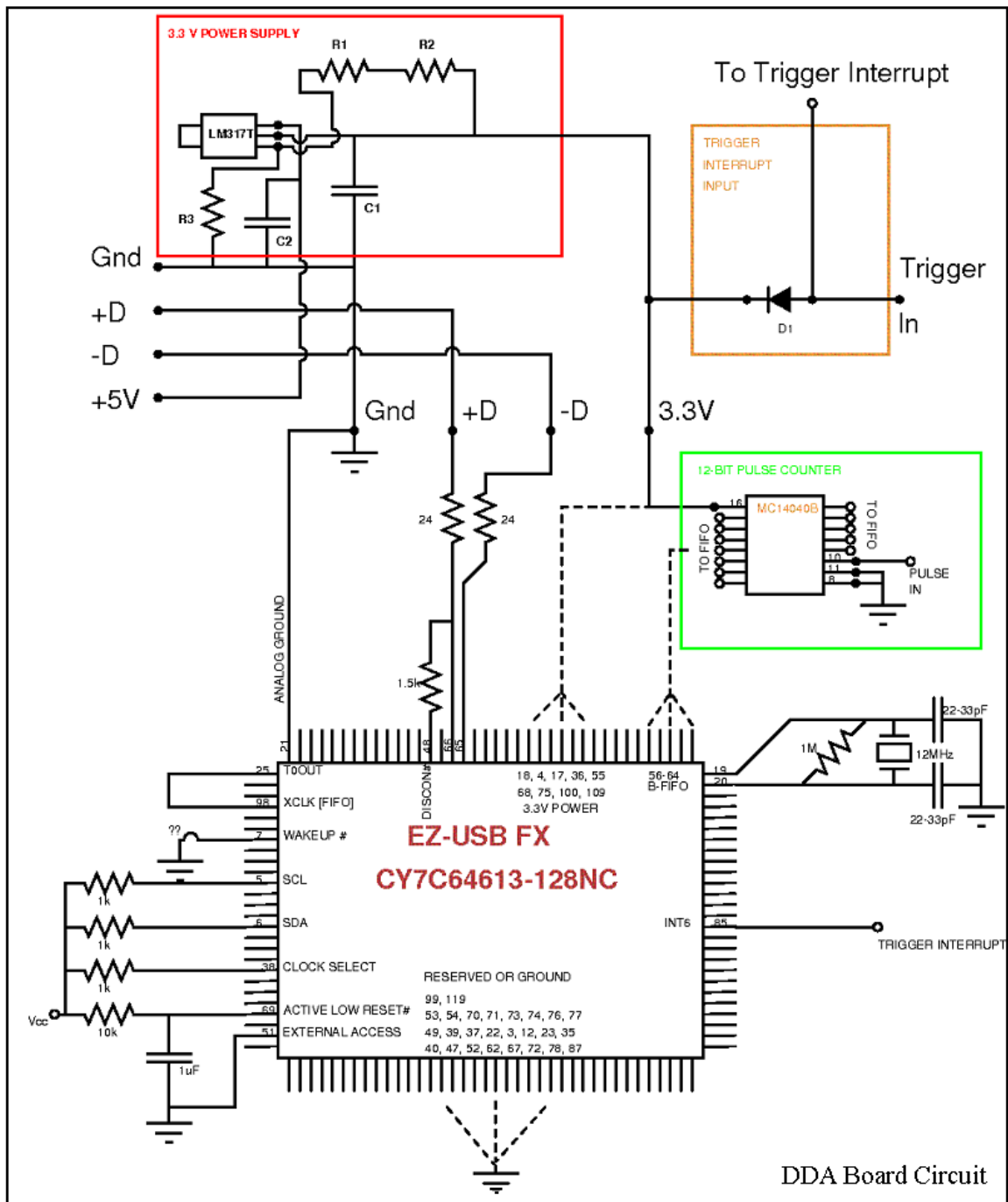
- Ah Q.R. Ahmad *et al.*, (2002), Phys. Rev. Lett. **89**.
- Al Alessandrello, A. *et al.*, (1988), Nuclear Phys. A **478**, 453-458
- As F.W. Aston, (1919), Rev. Sci. Instr., **18**, 739
- As F. W. Aston, (1919), *Phil. Mag.*, **38**, 707.
- As F.W. Aston, (1942), *Mass Spectra and Isotopes*, 2nd Ed., London, (Edward Aronold and Company).
- Au G. Audi, A.H. Wapstra, and C. Thibault, (2003), *The AME 2003 atomic mass evaluation*, Nucl. Phys., **A729**, 340
- Av F.T. Avignone, G.S. King, and Yu G. Zdesenko, (2005), New J. Phys. **7**, 6.
- Ba R.C. Barber, (1965), Can. J. Phys. **43**, p.716-721
- Ba R.C. Barber *et al.*, (1971), *A High Resolution Mass Spectrometer for Atomic Mass Determinations*, Rev. Sci. Instr., **42**, 1.
- Ba J. N. Bahcall, S. L. Glashow, (1987), *Upper limit on the mass of the electron neutrino*, Nature, **326**, 476 – 477.
- Ba D. Barillari, (1999), *Precision Mass Measurements of Some Isotopes of Tungsten and Mercury for and Adjustment to the Mass Table in the Region A=184 to A=204*, PhD Thesis, Department of Physics, University of Manitoba.
- Be Bernabei, R.*et al.*, (2001), INFN/AE-01/19
- Be Bernabei, R. *et al.*, (2002), Phys. Lett. **B546**, 23-28.
- Be Bernabei, R. *et al.*, (2003), (INFN), *Beyond the Desert*, Springer, p.365
- Be Bernabei, R. *et al.*, (2006), Eur. Phys. J. A Vol.27, Iss.2, p.35-41
- Bi R.T. Birge, (1932), Phys. Rev., **40**, 207.
- Bi R.L. Bishop, (1969), *Atomic Mass Differences for Some Rare Earth Isotopes Near N=90*, PhD Thesis, Department of Physics, University of Manitoba.

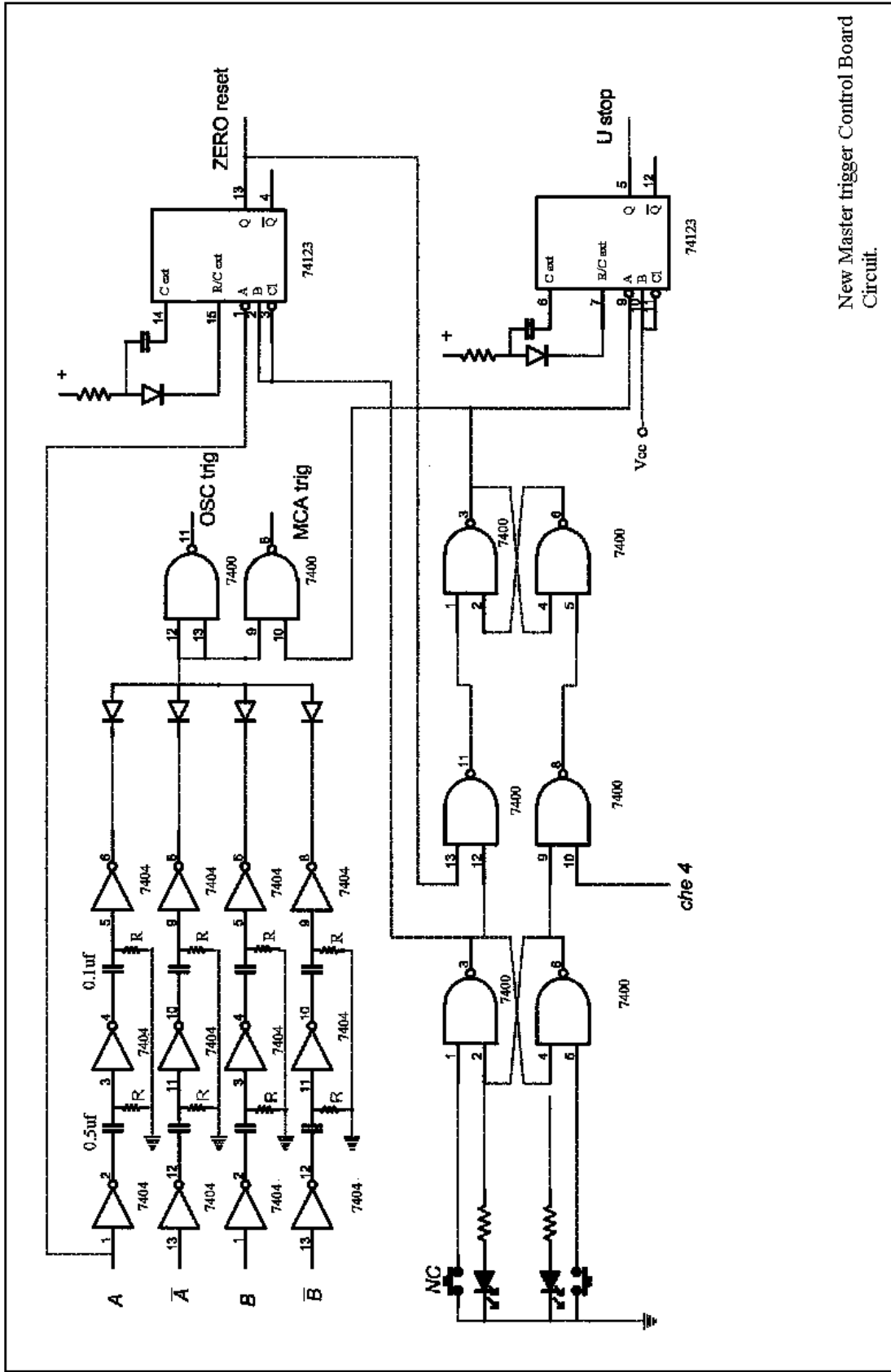
- Bi R.L. Bishop and R.C. Barber, (1970), *A High Precision Ratio Potentiometer*, Rev.Sci.Instr., **41**, 327.
- Bl W. Bleakney, (1936), *The Mass Spectrograph and Its Uses*, American Physics Teacher, **4**, 12.
- Ca B. Caccianiga and M. G. Giammarchi, (2000), *Astropart. Phys.* **14** 15
- Co Coggeshall, (1947), *F.Appl. Phys.*, **18**, 855.
- De A. J. Dempster, (1918), *A New Method of Positive Ray Analysis*, Phys. Rev., **11**, 316–325.
- Du H.E. Duckworth, R.C. Barber, and V.S. Venkatasubramanian, (1986), *Mass Spectroscopy*, 2nd edition, (Cambridge).
- Ei A. Einstein, (1905), *Annalen der Physik*, **18**, 639
- EXO SLAC-PUB-12399, (2006), *Searching for Double Beta Decay with the Enriched Xenon Observatory*, Prepared for CIPANP 2006: 9th Conference on the Intersections of Particle and Nuclear Physics, Carter Hall, for the EXO collaboration.
- Fi E. Fiorini, (2003) *Nuclear Phys.* **A721**, 171-181
- Fu Y. Fukuda *et al.*, (1998) *Phys. Rev. Lett.* **81**, 1562-1567.
- Ga Ju. M. Gavriljuk, V.V. Kuzminov, N. Ya. Osetrova, S.S. Ratkevich, (2000), *Phys. Rev.* **C61**, 035501
- Ga Ju. M. Gavriljuk, A. Gangapshev, V.V. Kuzminov, S. Panasenko, S. Ratkevich, (2006), *Physics of Atomic Nuclei*, Volume 69, Number 12, 2129-2133
- He A. Herlet *et al.*, (2006), *International Journal on Mass Spectrometry*, Vol. **251**, 131-137.
- He R. Herzog, (1934), *Zeitschrift fur Physik*, **89**, 447.
- Hi H. Hintenberger and L.A. König, (1959), *Mass Spectrometers and Mass Spectrographs Corrected for Image Defects*, *Advances in Mass Spectroscopy*, p.16, J.D.Waldron, ed., (Pergamon Press , London).
- Hy J.G. Hykawy, (1991), *Precise Determination of the ⁷⁶Ge-⁷⁶Se Atomic Mass Difference and the Majorana Mass of the Electron Neutrino*, PhD Thesis, Department of Physics, University of Manitoba.

- Is M.A.Islam, T.J.Kennett, W.V.Prestwich, (1990), *M1 and E2 Strength Functions of Barium from Thermal Neutron Capture*, Phys.Rev., **C42**, 207.
- KB K.T. Bainbridge, (1933), *Comparison of the Masses of He and H¹ on a Mass-Spectrograph*, Amer. Phys. Rev. **43**, 103 – 105.
- Ke L. Kerwin, (1963), *Mass Spectroscopy*, ed. By C.A. McDowell, p.104., New York, San Francisco, Toronto, and London, McGraw Hill.
- Ki T. Kirsten, H. Richter, E. Jessberger, (1983), Phys. Rev. Letters, **50**, 474.
- Kl H.V. Klapdor-Kleingrothaus, A. Dietz, L.Baudis, G. Heusser, I.V. Krivosheina, B. Majorovits, H. Paes, H. Strecker, A Balysh, A. Bakalyarov, S.T. Belyaev, V.I. Lebedev, and S. Zhukov, (2001), *Latest results from the HEIDELBERG-MOSCOW double beta decay experiment*, Eur. Phys. J., **A12**, 147-154.
- Ko K.S. Kozier, (1977), *Atomic Mass Determinations for Some Isotopes of Ti, W, and Hg*, PhD Thesis, Dept. of Physics, University of Manitoba.
- KoH L.A. König and H. Hintenberger, (1955), Z. Naturf. **10a**, 877.
- Lu R. Luescher, J. Farine, F. Boehm, *et al.*, (1998), Phys. Lett. **B434**, 407.
- Ma J. Mattauch, (1934), *Zur Systematik der Isotope*, Z. Physik. **91**, 361-371.
- Ma J. Mattauch, (1960), *Proceedings of the International Conference on Nuclidic Masses*, ed. Duckworth H.E., Toronto: University of Toronto Press, p.3.
- Me J.O. Meredith, F.C.G. Southon, R.C. Barber, P.Williams, H.E. Duckworth, (1973), IJMPD, **10**, 359.
- Mo P.J. Mohr and B.N. Taylor, (2005), Rev. of Mod. Phys. **77**
- Mo S. Moriyama (2001), For the XMASS collaboration *Proc. Int. Workshop on Techniques and Applications of Xenon Detectors (Tokyo, Japan, 3-4 December)* (Singapore: World Scientific) p 123
- Ni A. Nier, (1940), Rev. Sci. Instrum., **11**, 212.
- Os S. M. Oser & SNO Collaboration, (2003), Nuclear Physics B - Proceedings Supplements, **117**, 3-7.

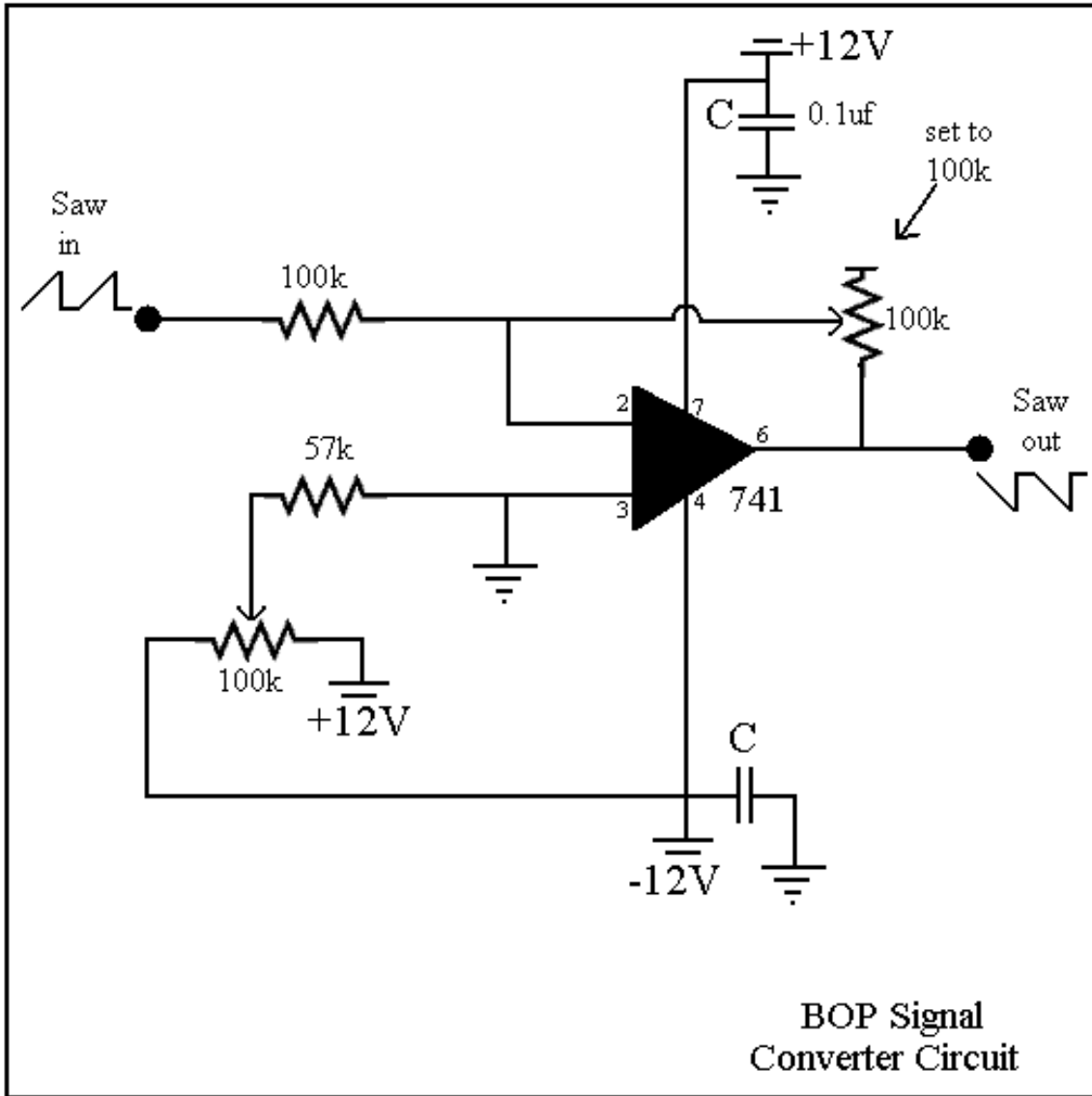
- Pa S.Pascoli, S.T. Petcov, and T. Schwetz, (2005), *The Absolute Neutrino Mass Scale, Neutrino Mass Spectrum, Majorana CP-Violation and Neutrinoless Double-Beta Decay*, CERN-PH-TH/2005-082.
- Re M. Redshaw, E. Wingfield, J. McDaniel, & E.G. Myers, (2007), *Phys. Rev. Lett.* **98**, 053003.
- Sa Savard, Guy; R. C. Barber, C. Boudreau, F. Buchinger, J. Caggiano, J. Clark, J. E. Crawford, H. Fukutani, S. Gulick, J. C. Hardy, A. Heinz, J. K. P. Lee, R. B. Moore, K. S. Sharma, J. Schwartz, D. Seweryniak, G. D. Sprouse and J. Vaz, (2004), *The Canadian Penning Trap Spectrometer at Argonne, Hyperfine Interactions*, Springer Netherlands, **132** (1-4), 221-228.
- Sh K.S. Sharma *et al.*,(1995), *The Canadian Penning Trap Mass Spectrometer*, p.811, in Proceedings of **ENAM'95**, International Conference on Exotic Nuclei and Atomic Masses, Arles, France, 1995, M. De Saint Simon and O. Dorlin, eds.
- Sh K.S. Sharma *et al.*, (1998), *Status of the Canadian Penning Penning Trap Mass Spectrometer at the Argonne National Laboratories*, p.130, in Proceedings of **ENAM'98** (see above)
- Si F. Simkovic, P. Domin, A. Faessler, (2002), arXiv:hep-ph/0204278v1
- So F.C.G. Southon (1973), Ph.D Thesis, University of Manitoba.
- St Stefan Söldner-Rembold on behalf of the NEMO 3 and SuperNEMO Collaborations, (2008), *Search for Neutrinoless Double Beta Decay with NEMO 3 and SuperNEMO*, Journal of Physics: Conference Series, **110**, 082019.
- Th J.J. Thomson, (1913), *Rays of positive electricity*, Proceedings of the Royal Society, **A89**, 1-20.
- Tr V.I. Tretyak, Y.G. Zdesenko, (2002), *Atomic Data & Nuclear Data Tables*, **80**, 83-116.
- Vu J.L. Vuilleumier *et al.*, (1993), *Phys. Rev.* **D48**, 1009.
- We Ch. Weinheimer, B. Degen, A. Bleile, J. Bonn, L. Bornschein, O. Kazachenko, A. Kovalik, E.W. Otten, (1999), *Phys. Lett.*, **B460**, 219.

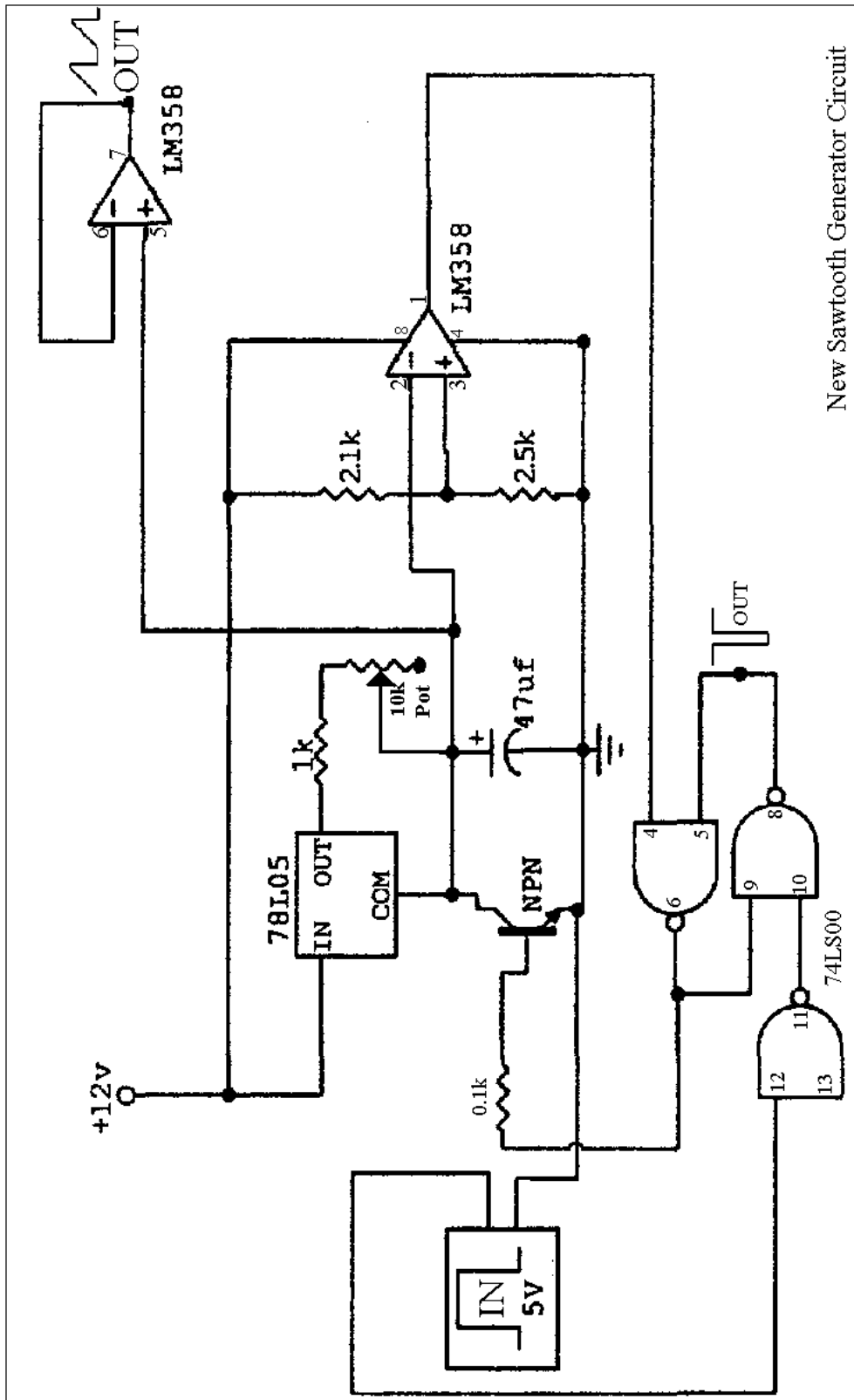
Appendix A - Circuits





New Master trigger Control Board
Circuit.

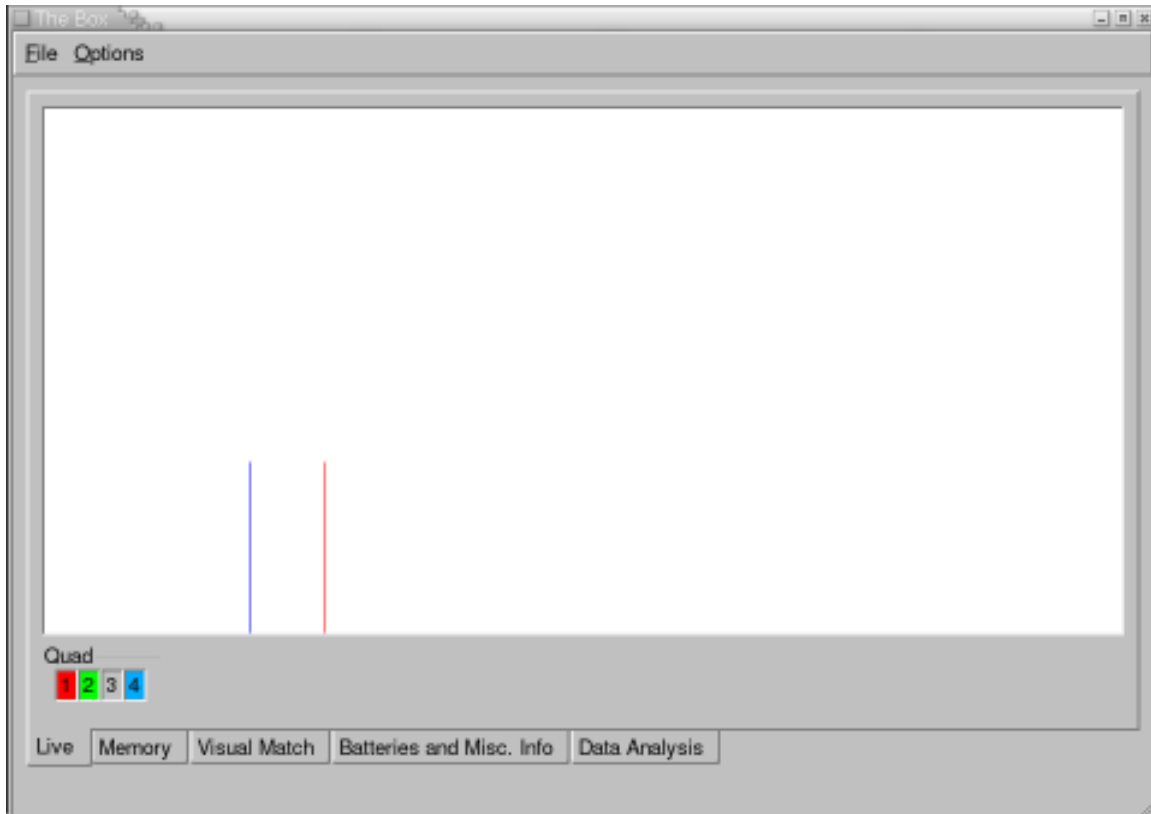




New Sawtooth Generator Circuit

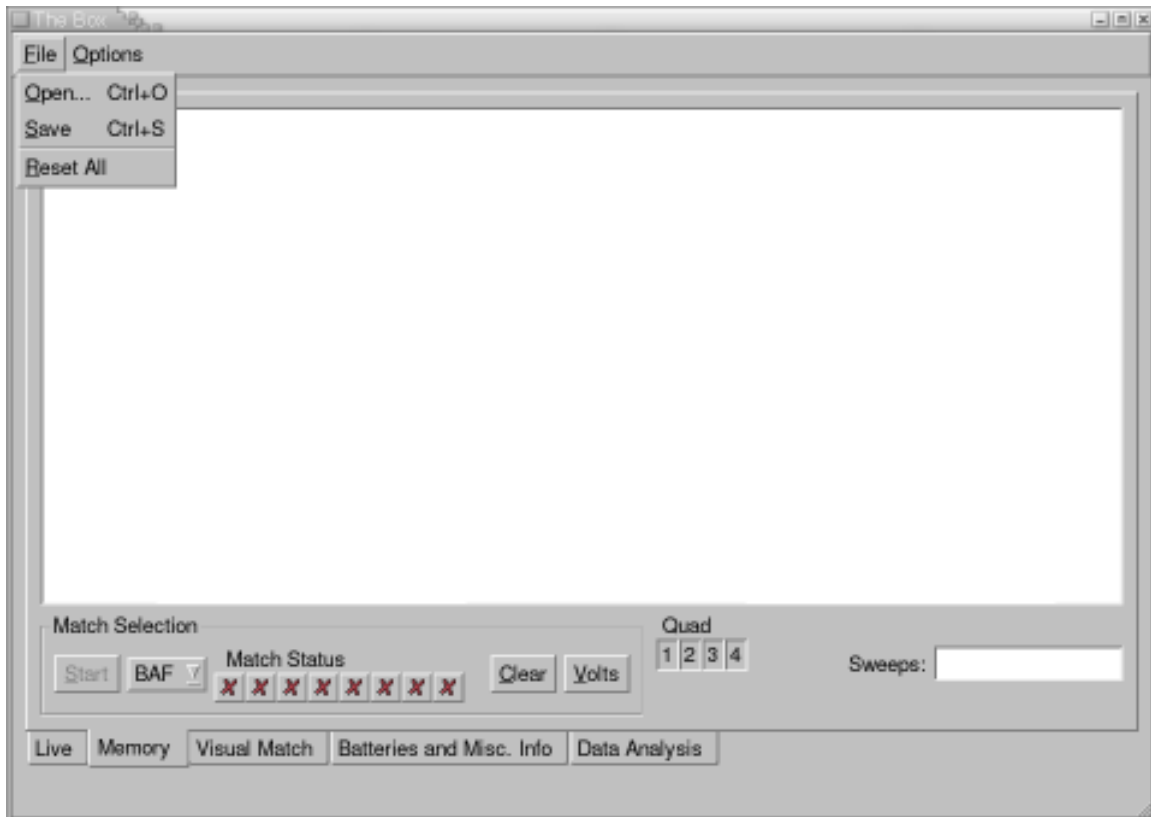
Appendix B – The *Analyzer* Program User Guide

Before starting up the program one should make sure that all cables going into and out of the DDA box are securely connected. When clicking the ‘Bomb’ icon on the bottom of the screen one should immediately see the following window pop-up:



If the channeltron power supply is on, noise spikes will be seen on the **Live** display. The default screen for the program is **Live**. It should be noted for clarity, that each quadrant has been designated with its own color. Even though quadrants in the program are numbered 1-4, they represent the true digital quadrants of 0-3. The user can also click on any **Quad** number button to remove it from the viewer (in which case the button looks like it is sticking out) or add it to the viewer (in which case it looks pressed). This is helpful when deciphering a problem of timing or voltage within a certain quadrant.

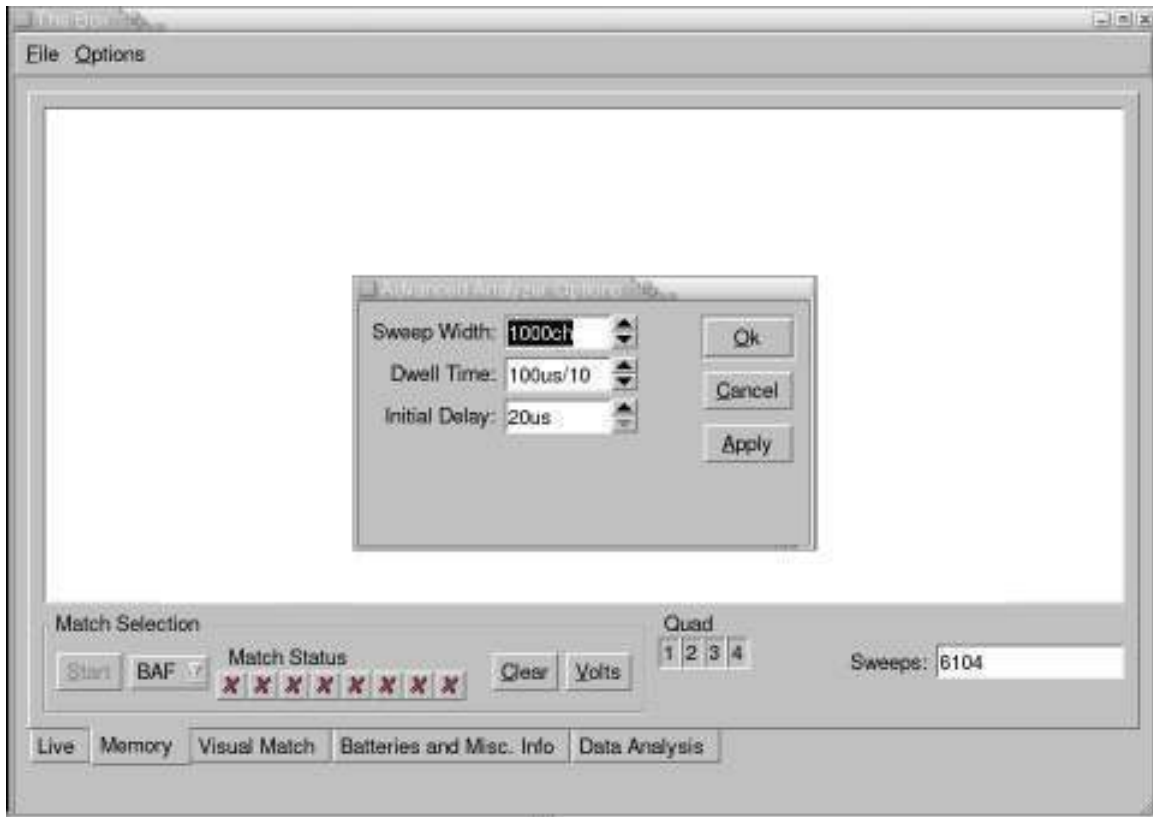
Clicking on the **File** button gives two options:



Open will allow you to open any previous worked on *.betsy file. A *.betsy file extension is the default file type used by the *Analyzer* program. **Save** will allow the user to save their file to either a *.betsy file or an AMDprime ready *.dat file by typing in the desired extension to the end of the filename. **Reset all** resets any presets and memory you have stored in your present work.

Saving to a *.dat file without filling in all the **Volts** fields will yield zeros or impracticable values for those fields.

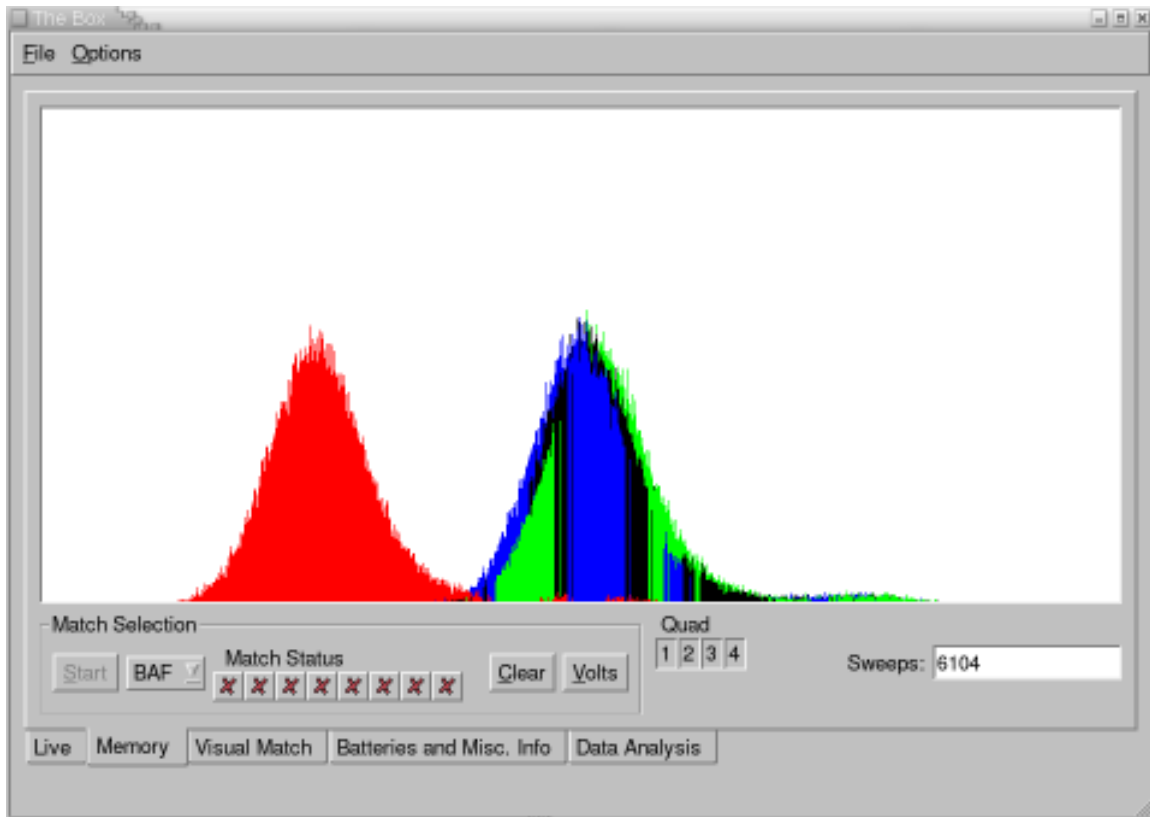
Clicking on the **Options** window gives you:



This will allow you to set the **Sweep Width** (to a max of 1024), the **Dwell Time** (usually 15 μ s) and the **Initial Delay** (anywhere between 10-20 μ s).

One can also choose a **Dot Display** or **Line Display** for window viewing under the **Options** menu

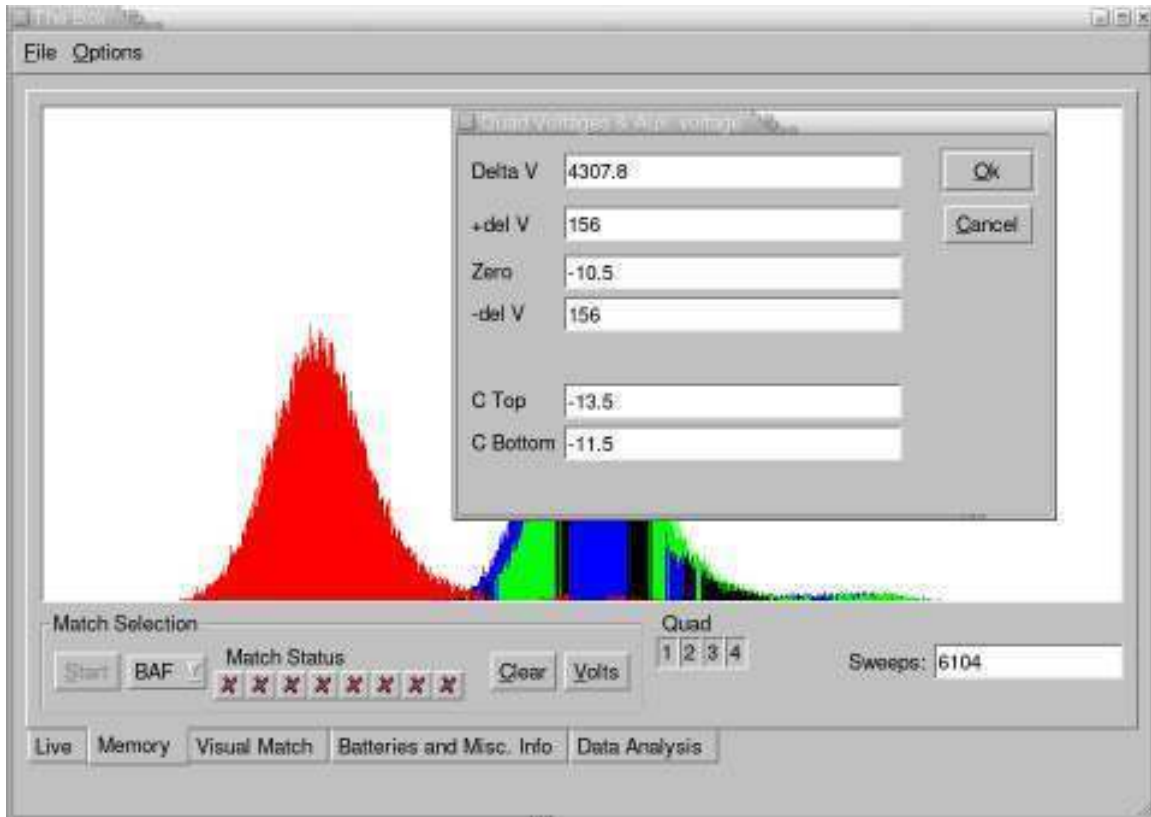
Next the **Memory** view with an accumulated peak (example) in **Line Display** mode is:



Here you can see the accumulated data for a BAF mode measurement. The **Sweeps** field stores the number of sweeps (remember that this is a full sweep of all 4 quadrants). The **Start/Stop** button starts the acquisition of data and stops it. The **Memory** view constantly re-scales the amplitude axis as more and more data is acquired; in other words it always fits the best image to the window.

The pull down menu to the right of the **Start/Stop** button allows the user to choose which of the 8 configurations (NAF, BAR...) to record the present data in. The **Match Status** buttons will show a ✓ for a completed configuration run or a ✗ for a non-completed one. Clicking on these buttons will display what memory, if any, has been saved to that mode. The **Clear** button clears all data on the selected **Match Status** configuration, including its **Volts** data.

The **Volts** button, when pressed, gives you:



The pop-up box that appears gives you six boxes to fill with voltage data. All the data should be in μBp units (see §4.4). **Delta V** is the large ΔV while $\pm\text{del V}$ are the respective split voltages (δV). The **C Top**, **C Bottom**, and **Zero** fields should be filled in as follows:

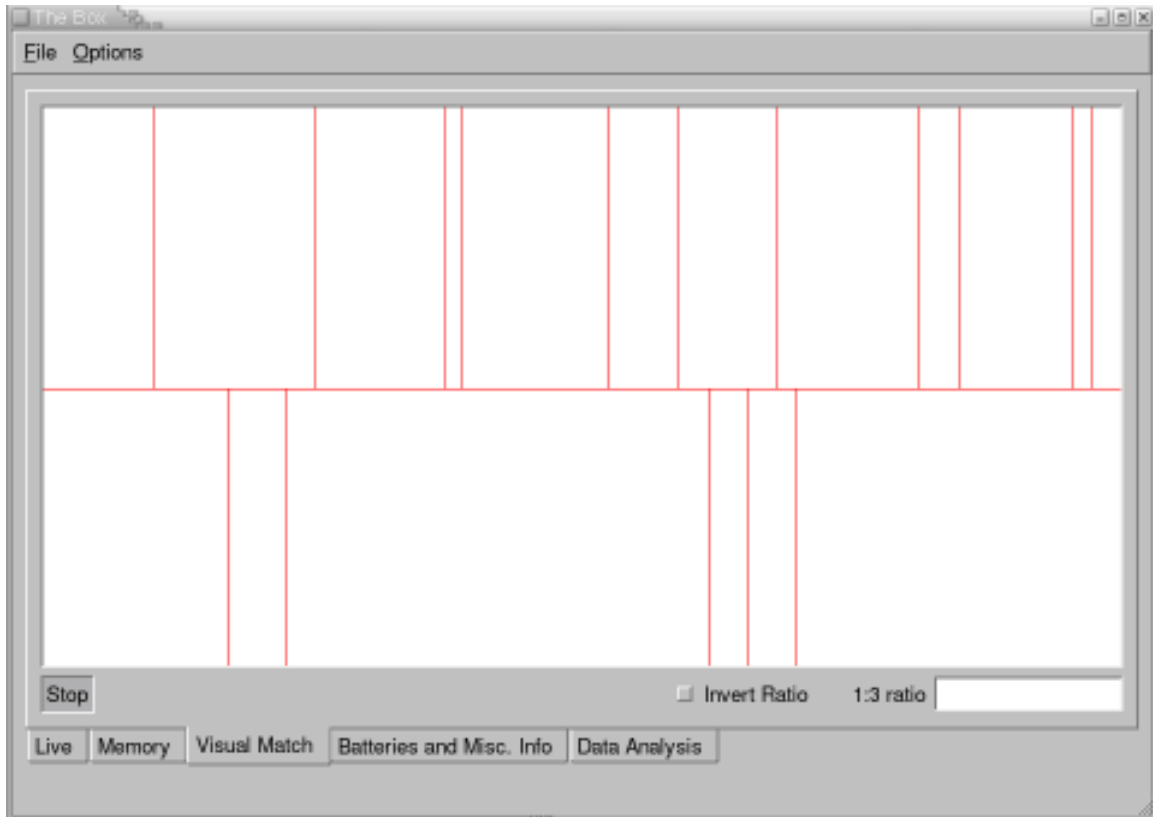
$$C_{\text{Top}} = T_{\text{F}} + T_{\text{R}} \quad C_{\text{Bot}} = B_{\text{F}} + B_{\text{R}}$$

$$P_{\text{F}} = T_{\text{F}} + B_{\text{F}} \quad P_{\text{R}} = T_{\text{R}} + B_{\text{R}}$$

Where T and B are the respective thermal emf's measured by the null potentiometer in the forward and reverse mode orientation (top and bottom plate of the ESA).

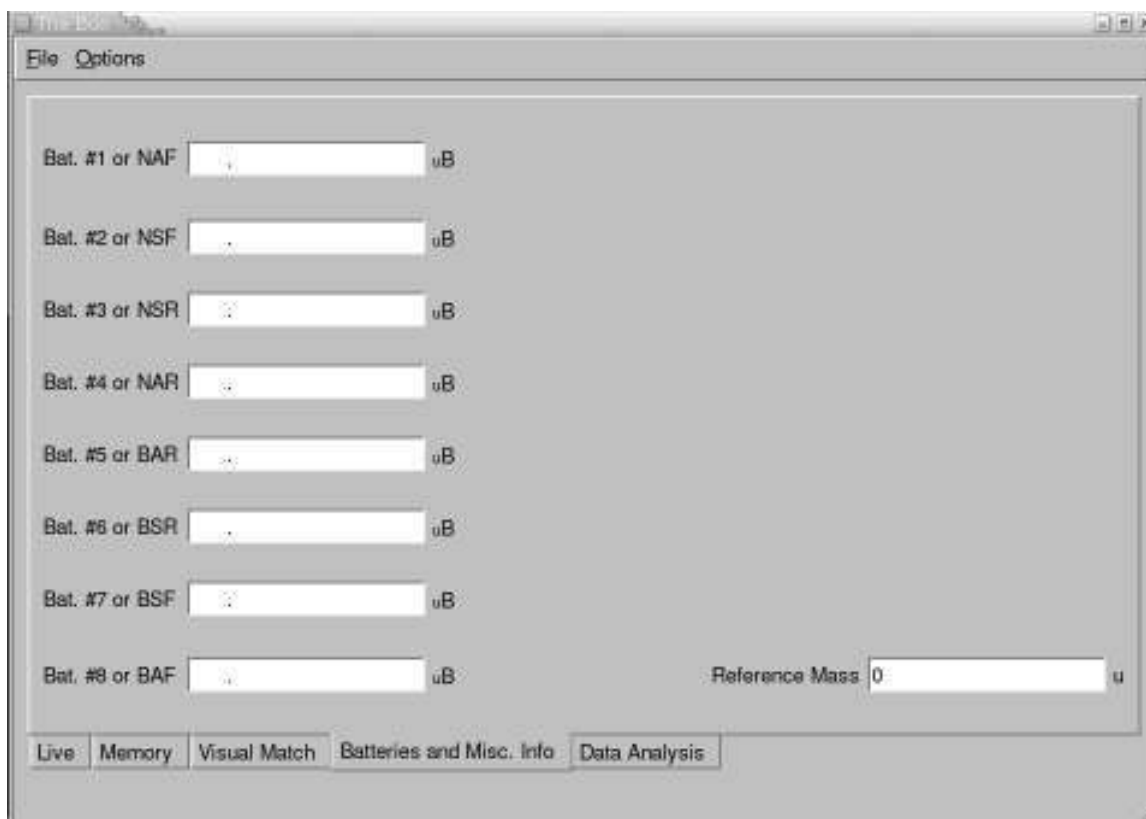
If in an 'Add' configuration, then **Zero** = P_{f} . If in a SUB configuration, then **Zero** = P_{R} . Every configuration has its own specific set of **Volts** data. Pressing any of the match status buttons brings up the stored acquired memory and pressing the **Volts** button in that configuration brings up the entered or not entered voltage data.

Clicking on the **Visual Match** tab gives the screen:



We have a **Start/Stop** button to accumulate data to memory. There is also a **ratio** field box that allows the user to enter the peak ratio to equalize the amplitudes of the matching peaks. In the above image you can see the noise peaks of a visually matched peak above and below the center line.

Clicking on the **Batteries and Misc. Info** tab gives:



The screenshot shows a window titled "Options" with a menu bar containing "File" and "Options". The main area contains eight input fields, each labeled with a battery number and its corresponding code: "Bat. #1 or NAF", "Bat. #2 or NSF", "Bat. #3 or NSR", "Bat. #4 or NAR", "Bat. #5 or BAR", "Bat. #6 or BSR", "Bat. #7 or BSF", and "Bat. #8 or BAF". Each field is followed by the unit "uB". To the right of these fields is a "Reference Mass" field with the value "0" and the unit "u". At the bottom of the window, there are five tabs: "Live", "Memory", "Visual Match", "Batteries and Misc. Info", and "Data Analysis". The "Batteries and Misc. Info" tab is currently selected.

Here you can enter the 8 battery values measured by the potentiometer, in μBp units (the program denotes these units as uB), as well as your reference mass used for calibration, in normal 'u' units (see §5.2).

All of the voltage input fields should be and can be filled in at any time during or after the measurement, or at a later time by reopening a saved *.betsy file.

The files can then be saved to an analyzer *.betsy file or an AMDprime ready *.dat file.

Troubleshooting

If for any reason the Analyzer program fails to boot, does not read in any channeltron counts, or work in any fashion, please follow the following steps in numerical order:

- 1) Make sure all cords are plugged in to the Box. If all connections are secure:
 - a) Close Analyzer program on the PC, restart the PC.
 - b) un-plug USB cable from the Box, wait one minute, then plug back into the box
 - c) Start up analyzer program

If the program still does not work proceed to step 2.

- 2) To restart the Analyzer 'Server', type the following in a Linux Terminal:

```
sudo killall analyzerd  
sudo /etc/init.d/analyzerd start
```

The password asked is just 'pete'.

If the above does not fix the problem, restart the computer; restarting will reload the kernel drivers.

Finally, if the device still refuses to function, you can manually reload the firmware into the box by typing the following into a Terminal:

```
ssh root@box  
password: ~tyop* or pete  
killall server  
rmmod box  
ls /proc/bus/usb/001
```

(you should now see a list of numbers like 001, 002, 005,...etc. Let NUM = the largest number)

```
sudo fxload -t fx -D /proc/bus/usb/001/NUM -I  
/usr/lib/hotplug/firmware/analyzer.ihx
```

Then close the terminal and restart the analyzer.

Appendix C-1: *Analyzer* Source Code

The following code is for the data collection which is downloaded to the Cypress CY7C64613-128NC microcontroller chip at every PC reboot or restart of the *Analyzer* Program:

```
.module Analyzer
.include 'driver.inc'
.include 'analyzer.inc'

.area DSEG (DATA)
dwell_time: .db 0x0f ; loops delay (~10us)
channel_cnt_lo: .db 0xe8 ; 1000 channels sweep width
channel_cnt_hi: .db 0x04
initial_delay: .db 0x0f ; 10us delay
cur_quad: .db 0x00 ; cur quad

.area CSEG (CODE)

;; -----
;; -- getAnalyzer
;;
;; INPUT:
;; DPTR - beginning ISO buffer 1001 bytes long
;;
;; OUTPUT:
;; none
;;
;; All channel data is to be taken and stored every 10µs (60 cycles)
;; R0 contains the rolling sum (FIXME: not used...)
;; R1 contains channels remaining LOWBYTE
;; R2 contains prev. byte
;; R3 used as general delay "timer"
;; R4 = channel dwell time
;; R5 contains channels remaining HIBYTE (3 is 4 since using djnz and zero means 0 in
lowbyte as well)
;;

getAnalyzer:
acall preStartCheck
clr A
mov R2, TL0

2000$:
nop ; (1) padding to get even µs delay
nop ; (1)
nop ; (1)

2001$:
mov A, TL0 ; (2) get current count
nop ; (1) padding for "even" µs delay
mov R3, A ; (1) save for later
clr c ; (1) clear carry flag so we subtract correctly
subb A, R2 ; (1)
movx @DPTR, A ; (2) move to ISO
mov A, R3 ; (1)
mov R2, A ; (1) store count in R2
mov A, R4 ; (1) channel dwell time
mov R3, A ; (1)
2001$: djnz R3, 2001$ ; (3)*"15"="45" filler
; total time = 12+3+dwell_time*3 = [3µs, 130.5µs]/ch

djnz R1, 2000$ ; (3) low_byte count down
djnz R5, 2001$ ; (3) high byte count down

;; each sweep is terminated by FF FF FF
```

```

mov     A, #0xFF
movx   @DPTR, A
movx   @DPTR, A
movx   @DPTR, A
ret

;; -----
;; -- preStartCheck
;;
;; Initializes the next analyzer run. Checks for RESET signal [ie.
;; the first quad]. Also checks if the buffer is empty. Also it
;; introduces a delay of 600 cycles [100 µs or 10 channels]
;;
;; INPUT:
;;           none
;;
;; OUTPUT:
;;           DPTR - beginning of ISO buffer
;;

preStartCheck:
inc     DPS                ; (1) we leave with original DPTR being IN8DATA
mov     DPTR, #cur_quad    ; (3) loads current quad address
jnb    IOB5, 1001$        ; (2) check if reset was called

clr     A                  ; (1) resets the current quad
ajmp   1002$              ; (3)

1001$:
movx   A, @DPTR           ; (2)
nop
nop                          ; (2) wait 2 instruction cycles as above

1002$:
;; Load DPTR with the FIFO buffer position and get ready to
;; move some data
;;
inc     DPS                ; (1)
mov     DPTR, #IN8DATA    ; (3)
movx   @DPTR, A          ; (2) move current quad into in buffer
inc     A                  ; (1)
inc     DPS                ; (1)
movx   @DPTR, A          ; (2)

;; get channel width
mov     DPTR, #dwell_time
movx   A, @DPTR
mov     R4, A

;; get sweep width
mov     DPTR, #channel_cnt_lo
movx   A, @DPTR
mov     R1, A

mov     DPTR, #channel_cnt_hi
movx   A, @DPTR
mov     R5, A

;; load the initial delay into R0
mov     DPTR, #initial_delay
movx   A, @DPTR
mov     R0, A

;; get back to pointing DPTR to IN8DATA
inc     DPS                ; (1)

;; need to wait for the "initial_delay"/3 µs for stability
1003$:
djnz   R0, 1003$
ret

```

```

;; processRequests reads the current request on EP1OUT. The request consists of
;;
;; <REQUEST> <req. data>
;; where REQUEST is always one byte long
;;
;; All of the valid requests are in the Documentation.txt
;;
;;
processRequests:
    mov     DPTR, #OUT1BC          ;; check for _valid_ requests
    movx   A, @DPTR
    jz     processRequests_ret

    mov     DPTR, #OUT1BUF        ;; read the request
    movx   A, @DPTR
    inc    DPTR

    mov     DPTR, #processRequests_table
    anl   A, #0x03                ;; allow for (4) requests only
    mov    B, #4
    mul   AB
    jmp   @A+DPTR

processRequests_table:
    acall  _processRequests_setChannelSize
    sjmp  processRequests_ret

    acall  processRequests_getChannelSize
    sjmp  processRequests_ret

    acall  processRequests_setSweepWidth
    sjmp  processRequests_ret

    acall  processRequests_getSweepWidth
    sjmp  processRequests_ret

processRequests_ret:
    clr   A
    mov   DPTR, #OUT1BC
    movx @DPTR, A                ;; make sure we always rearm the EP1 OUT

    ret

;; processRequests_* functions are located here
processRequests_setChannelSize:
    mov   DPTR, #OUT1BUF+1
    movx A, @DPTR
    mov   DPTR, #dwell_time
    movx @DPTR, A
    ret

processRequests_getChannelSize:
    mov   DPTR, #dwell_time
    movx A, @DPTR
    mov   DPTR, #IN1BUF
    movx @DPTR, A
    mov   A, #1
    mov   DPTR, #IN1BC
    movx @DPTR, A
    ret

processRequests_setSweepWidth:
    mov   DPTR, #OUT1BUF+1        ; copy the high-byte first
    movx A, @DPTR
    inc  A                        ; must be 1 more since we dec. before jump

```

```

mov     DPTR, #channel_cnt_hi
movx   @DPTR, A

mov     DPTR, #OUT1BUF+2      ; and now the low-byte
movx   A, @DPTR
mov     DPTR, #channel_cnt_lo
movx   @DPTR, A

ret

processRequests_getSweepWidth:
; ; We return the sweep width high-byte first, 2 byte total
mov     DPTR, #channel_cnt_hi
movx   A, @DPTR
dec     A                      ; we need to decrement by 1 to get true 256 multiple
mov     DPTR, #IN1BUF
movx   @DPTR, A

mov     DPTR, #channel_cnt_lo
movx   A, @DPTR
mov     DPTR, #IN1BUF+1
movx   @DPTR, A

mov     A, #2
mov     DPTR, #IN1BC
movx   @DPTR, A
ret

```


Appendix C-2: *Analyzer* Main Code

This code is required for the *Analyzer* program, on a LINUX based PC, to communicate with the DDA box, connected via a USB cable:

```
.module Main
.include 'driver.inc'
.include 'analyzer.inc'

;; Initial jump table for interrupt handlers
;; Let's begin to crack some code - in 1st memory block
.area CSEG (CODE)
;; first, we need to generate an interrupt table
;; first main jump is 3 bytes and all interrupts after that
;; are 8 bytes each!
ljmp MAIN
ljmp INT0_HANDLER ; Int#0 Pin
    .dw 0
    .dw 0
    .db 0
ljmp TIMER0_OVERFLOW ; Timer 0 Overflow
    .dw 0
    .dw 0
    .db 0
ljmp INT2_HANDLER ; Int#1 Pin
    .dw 0
    .dw 0
    .db 0
ljmp TIMER1_OVERFLOW ; Timer 1 Overflow
    .dw 0
    .dw 0
    .db 0
ljmp UART0 ; Interrupt from UART 0
    .dw 0
    .dw 0
    .db 0
ljmp TIMER2_OVERFLOW ; Timer 2 Overflow
    .dw 0
    .dw 0
    .db 0
ljmp RESUME ; Wakeup# pin or USB Core Interrupt
    .dw 0
    .dw 0
    .db 0
ljmp UART1 ; Interrupt from UART 1
    .dw 0
    .dw 0
    .db 0
ljmp USB ; USB Interrupt - a second interrupt table
    ; must be generated since using Autovectoring
    .dw 0
    .dw 0
    .db 0
ljmp I2C ; I2C Interrupt
    .dw 0
    .dw 0
    .db 0
ljmp FIFO ; FIFO Interrupt - Int#4 Pin in our case
    .dw 0
    .dw 0
    .db 0
ljmp INT5_HANDLER ; Int#5 Pin [active LOW!]
    .dw 0
    .dw 0
    .db 0
ljmp INT6_HANDLER ; Int#6 Pin
```

```

        .dw      0
        .dw      0
        .db      0                ; last one not needed
;; NOTE: Using a weak compiler so the next thing is hardcoded
;;       as 0x100-0x6b=0x95

;; The jump table must be at a page boundary (eg. 0100h) so the
;; easiest thing to do is waste some memory here.
        .ds 0x95

USB:                                ; USB Interrupt - a second interrupt table
                                    ; must be generated since using Autovectoring

ljmp    SUDAV_ISR
nop
ljmp    SOF_ISR
nop
ljmp    SUTOK_ISR
nop
ljmp    SUSPEND_ISR
nop
ljmp    USBRESET_ISR
nop
ljmp    IBN_ISR
nop
ljmp    EP0IN_ISR
nop
ljmp    EP0OUT_ISR
nop
ljmp    EP1IN_ISR
nop
ljmp    EP1OUT_ISR
nop
ljmp    EP2IN_ISR
nop
ljmp    EP2OUT_ISR
nop
ljmp    EP3IN_ISR
nop
ljmp    EP3OUT_ISR
nop
ljmp    EP4IN_ISR
nop
ljmp    EP4OUT_ISR
nop
ljmp    EP5IN_ISR
nop
ljmp    EP5OUT_ISR
nop
ljmp    EP6IN_ISR
nop
ljmp    EP6OUT_ISR
nop
ljmp    EP7IN_ISR
nop
ljmp    EP7OUT_ISR
nop

;; -----
;; void main (void)
;; - entry point to the program
;;

MAIN:
;; initially, we need to set proper stack frame!!!
mov     SP, #0x30

;; First, we need to initialize the USB chip properly

```

```

acall  initUSB

;; now, we need to initialize the Timer 0 for one time
;; count used to get the same offset from the beginning
;; of the trigger to the gathering of data. The analyzer
;; is called in the timer routine - highest priority!
mov    CKCON, #0b00111000; set all clocks to fast mode [1/4 cycles]
clr    A
mov    TMOD, #0b00110101 ; set Timer 0 Mode 1 clocked from pin
mov    TCON, #0b00010000 ; Timer 0 enable & disable the interrupts for now
mov    TLO, A
mov    TH0, A

;; Now, we need to enter an event loop to properly
;; handle requests from the host, as well as to
;; operate the devices in a reasonably interrupt free
;; fashion. This means that while doing proper timings
;; in the code, the interrupts MUST remain suspended.
;; Hopefully the USB core can handle that!!

loop:
;; All requests from the host are processed here. ProcessRequests
;; returns after processing ONE (1) request from the host.
;; Requests that cannot be satisfied at the moment, are
;; left alone until they can be filled. This leaves
;; the request endpoint stuck

; first, let's wait for the trigger..
jnb    IOB6, loop

acall  getAnalyzer

acall  processRequests      ;; processes one request here if any
sjmp  loop

;; -----
;; -- void initUSB (void)
;;
;; Initializes all of the required registers and
;; renumerates the USB chip.
;;
;; Preserves all registers except A, R0

initUSB:

clr    A                    ; used to clear all of the external memory things
mov    PSW, A               ;
mov    DPS, A               ; select first data pointer (DPTR0) as DPTR
mov    CKCON, A             ; no external wait states and reg. timer
mov    IE, A                ; disable all interrupts
mov    EIE, A

mov    DPTR, #USBCS
movx   @DPTR, A             ; disconnect from USB bus !!!!

clr    A
mov    DPTR, #IN07IEN
movx   @DPTR, A             ; disable all IN interrupts
mov    DPTR, #OUT07IEN
movx   @DPTR, A             ; disable all OUT interrupts

mov    A, #0b00000010
mov    DPTR, #IN07VAL
movx   @DPTR, A             ; enable EP1 IN
mov    DPTR, #OUT07VAL
movx   @DPTR, A             ; enable EP1 OUT

;; clear all endpoint dataX toggles !!!!

```

```

        mov     R0, #0           ; R0 is the index
        mov     DPTR, #TOGCTL
toggle_loop:
        mov     A, R0           ; for(i=0;i<7;++i){
        orl     A, #0x10        ; TOGCTL=0x10 +i;
        movx    @DPTR, A        ; TOGCTL=0x30 +i;

        mov     A, R0           ; TOGCTL=i;
        orl     A, #0x30        ; TOGCTL=0x20 +i;
        movx    @DPTR, A        ; }

        mov     A, R0
        movx    @DPTR, A

        mov     A, R0
        orl     A, #0x20
        movx    @DPTR, A

        inc     R0
        cjne    R0, #8, toggle_loop

        clr     A
        mov     DPTR, #ISOCTL
        movx    @DPTR, A        ; enable ISO IN EP8
        mov     DPTR, #OUTISOVAL
        movx    @DPTR, A
        mov     DPTR, #INISOVAL
        mov     A, #0b00000001
        movx    @DPTR, A

;; we need to set ISO FIFO properly here - all are 0 except for IN EP8 which
;; is 1020 bytes long
        clr     A
        ;mov     DPTR, #OUT8ADDR
        ;movx    @DPTR, A        ; EP8 OUT
        ;mov     DPTR, #OUT9ADDR
        ;movx    @DPTR, A        ; EP9
        ;mov     DPTR, #OUT10ADDR
        ;movx    @DPTR, A        ; EP10
        ;mov     DPTR, #OUT11ADDR
        ;movx    @DPTR, A        ; EP11
        ;mov     DPTR, #OUT12ADDR
        ;movx    @DPTR, A        ; EP12
        ;mov     DPTR, #OUT13ADDR
        ;movx    @DPTR, A        ; EP13
        ;mov     DPTR, #OUT14ADDR
        ;movx    @DPTR, A        ; EP14
        ;mov     DPTR, #OUT15ADDR
        ;movx    @DPTR, A        ; EP15
        mov     DPTR, #IN8ADDR
        movx    @DPTR, A        ; EP8 IN
        ;add     A, 0x30
        ;mov     DPTR, #IN9ADDR
        ;movx    @DPTR, A        ; EP9
        ;mov     DPTR, #IN10ADDR
        ;movx    @DPTR, A        ; EP10
        ;mov     DPTR, #IN11ADDR
        ;movx    @DPTR, A        ; EP11
        ;mov     DPTR, #IN12ADDR
        ;movx    @DPTR, A        ; EP12
        ;mov     DPTR, #IN13ADDR
        ;movx    @DPTR, A        ; EP13
        ;mov     DPTR, #IN14ADDR
        ;movx    @DPTR, A        ; EP14
        ;mov     DPTR, #IN15ADDR
        ;movx    @DPTR, A        ; EP15

        mov     DPTR, #PORTSETUP

```

```

mov     A, #0b00000001
movx   @DPTR, A      ; enable using SFRs for I/O control
mov     DPTR, #USBIEN
mov     A, #0b00000001 ; was 0..011
movx   @DPTR, A      ; disable all USB interrupts but SOF and SUDAV

mov     A, #0b00010001
mov     DPTR, #USBBAV
movx   @DPTR, A      ; enable autovectoring

mov     DPTR, #USBPAIR
mov     A, #0b10000000
;clr   A
movx   @DPTR, A      ; turn off double buffering

mov     A, #0b00000110 ;; was 00000110
mov     DPTR, #USBCS

mov     EICON, #0b01000000 ; disable WAKEUP int
mov     EIE, #0b11100001 ; (was 0b11110001) enable USB interrupts and int 6
mov     IP, #0b10000000 ; make all normal int low priority
mov     EIP, #0b11110000 ; make all other int low except pin6 int
movx   @DPTR, A      ; reconnect to the USB bus and use our own USB control

;; reenumeration is complete here -----

clr     A

;; make all ports pin addressable and outputs except for PINS
mov     DPTR, #PORTACFG
movx   @DPTR, A
mov     DPTR, #PORTBCFG
movx   @DPTR, A
mov     DPTR, #IFCONFIG
movx   @DPTR, A
mov     DPTR, #PORTCCFG
;mov   A, #0b00110000 ; enable T0 and T1 pins
movx   @DPTR, A
clr     A

dec     A ; drive all pins low
mov     SOEA, A
mov     SOEB, #0b10001111
mov     SOEC, #0b11001111
mov     SOEE, A
clr     A
mov     SOED, A
mov     IOA, A
mov     IOB, A
mov     IOC, A
mov     IOE, A

mov     DPTR, #OED
movx   @DPTR, A

;mov   IOD, A

;; enable all interrupts
setb   EA
ret

;; -----
;; MAIN INTERRUPT ROUTINES - from the jump table
;;
;;
INT0_HANDLER: ; Int#0 Pin
TIMER0_OVERFLOW: ; Timer 0 Overflow
INT2_HANDLER: ; Int#1 Pin

```

```

TIMER1_OVERFLOW:          ; Timer 1 Overflow
UART0:                   ; Interrupt from UART 0
TIMER2_OVERFLOW:        ; Timer 2 Overflow
RESUME:                  ; Wakeup# pin or USB Core Interrupt
UART1:                   ; Interrupt from UART 1
I2C:                     ; I2C Interrupt
FIFO:                    ; FIFO Interrupt - Int#4 Pin as well
INT5_HANDLER:           ; Int#5 Pin
    reti

INT6_HANDLER:            ; Int#6 Pin
    ;; ok, the sweep has started so we need to get the data cracking
    ;; into the buffer - we want a delay of about 50 instructions
    ;; Also, we need to turn off the interrupts
    clr     EA
    push   ACC
    push   DPS
    push   DPH1
    push   DPL1
    push   DPH0
    push   DPL0
    mov    A, R0
    push   ACC
    mov    A, R1
    push   ACC
    mov    A, R2
    push   ACC
    mov    A, R3
    push   ACC          ; save DPTR, A, R0, R1, R2, R3

    acall  preStartCheck ; check if buffers are available and wait R0 time
    acall  getAnalyzer

    ;; clear int 6
    anl   EICON, #0b11110111

    ;; restore registers
    pop   ACC
    mov   R3, A
    pop   ACC
    mov   R2, A
    pop   ACC
    mov   R1, A
    pop   ACC
    mov   R0, A
    pop   DPL0
    pop   DPH0
    pop   DPL1
    pop   DPH1
    pop   DPS
    pop   ACC
    setb  EA          ; enable back the interrupts
    reti

    ;; -----
    ;; USB Interrupts
    ;;
    ;;SUDAV_ISR:
SOF_ISR:
    reti

SUTOK_ISR:
SUSPEND_ISR:
USBRESET_ISR:
IBN_ISR:                ; this one is reserved!!!
    push  ACC
    push  DPL
    push  DPH
    push  DPL1

```

```

push    DPH1
;; first, clear the USB (INT2) interrupt request
anl     EXIF, #0b11101000
mov     INT2CLR, A      ;; clear the irq

mov     DPTR, #USBIRQ
mov     A, #0b00000010
movx    @DPTR, A

;; return

pop     DPH1
pop     DPL1
pop     DPH
pop     DPL
pop     ACC
reti

EP2OUT_ISR:
push    DPS
push    DPL
push    DPH
push    DPL1
push    DPH1
push    ACC
mov     A, R0
push    ACC
mov     A, R1
push    ACC

;; clear the USB interrupt
anl     EXIF, #0b11101000; FIRST, clear the USB (INT2) interrupt req.
mov     INT2CLR, A

mov     DPTR, #OUT07IRQ ; clear the usb interrupt request
mov     A, #0b00000100
movx    @DPTR, A

;; read in the request byte from the buffer
mov     DPTR, #OUT2BUF
movx    A, @DPTR
mov     R1, A

cjne   A, #2, 222$      ; if not equal, jump to next intruction
222$:  jnc     ep2_out_ret ; Jump Greater Than instruction

;; clear all endpoint dataX toggles !!!!
mov     R0, #0          ; R0 is the index
mov     DPTR, #TOGCTL
ep2_out_datatoggle_loop:
mov     A, R0           ; for(i=0;i<7;++i){
orl     A, #0x10        ; TOGCTL=0x10 +i;
movx    @DPTR, A       ; TOGCTL=0x30 +i;

mov     A, R0           ; TOGCTL=i;
orl     A, #0x30        ; if(IN==1) TOGCTL=0x20 +i;
movx    @DPTR, A       ; }

mov     A, R0
movx    @DPTR, A

cjne   A, #1, 223$
sjmp   224$

223$:  mov     A, R0
orl     A, #0x20
movx    @DPTR, A

```

```

224$:
    inc     R0
    cjne   R0, #7, ep2_out_datatoggle_loop

ep2_out_ret:
    pop    ACC
    mov    R1, A
    pop    ACC
    mov    R0, A
    pop    ACC
    pop    DPH1
    pop    DPL1
    pop    DPH
    pop    DPL
    pop    DPS
    reti

EP0IN_ISR:
EP0OUT_ISR:
EP1IN_ISR:
EP1OUT_ISR:
EP2IN_ISR:
EP3IN_ISR:
EP3OUT_ISR:
EP4IN_ISR:
EP4OUT_ISR:
EP5IN_ISR:
EP5OUT_ISR:
EP6IN_ISR:
EP6OUT_ISR:
EP7IN_ISR:
EP7OUT_ISR:
    ;; first, clear the USB (INT2) interrupt request
    anl    EXIF, #0b11101000
    mov    INT2CLR, a        ;; clear the irq

    ;; return
    reti

```


Appendix C-3: *Analyzer Core Code*

This is the Setup-Interrupt routine that is used in response to the Host's Control requests:

```
.module usbControlHandler
.include 'driver.inc'
.include 'analyzer.inc'

.area CSEG (CODE)

AddAtoDPTR:
;; Adds A to DPTR and returns. Only A and C flag is affected
jz    AddAtoDPTR
inc   DPTR
dec   A
ajmp  AddAtoDPTR
AddAtoDPTRret:
ret

SUDAV_ISR:
;; save all registers
push  ACC
push  DPS
push  DPH1
push  DPH0
push  DPL1
push  DPL0
push  B
mov   A, R0
push  ACC

anl   EXIF, #0b11101111; FIRST, clear the USB (INT2) interrupt req.
mov   INT2CLR, A

;; clear the HSNACK bit
mov   DPTR, #EPOCS
movx  A, @DPTR
orl   A, #0b00000010
movx  @DPTR, A

;; let's handle our request using our request vector table
mov   DPTR, #SETUPDAT+1
movx  A, @DPTR
mov   DPTR, #SETUPDAT
cjne  A, #0x0C+1, aq
aq:   jnc   BadRequest      ; jump if request is beyond what we know

mov   B, #6                ; multiply offset by size of the vector
mul   ab
inc   DPS                  ; save setup pointer
mov   DPTR, #RequestVectorTable
jmp   @A+DPTR

RequestVectorTable:
inc   DPS                  ; size 2
acall GetStatus            ; size 2 -- bRequest=0x00
ajmp  EndOfRequestTable; size 2

inc   DPS
acall ClearFeature        ; bRequest=0x01
ajmp  EndOfRequestTable

inc   DPS
acall ZeroStall           ; bRequest=0x02
ajmp  EndOfRequestTable
```

```

inc     DPS
acall   SetFeature      ; bRequest=0x03
ajmp    EndOfRequestTable

inc     DPS
acall   ZeroStall      ; bRequest=0x04
ajmp    EndOfRequestTable

inc     DPS
nop                                           ; bRequest=0x05 -- core handled
nop
ajmp    EndOfRequestTable

inc     DPS
acall   GetDescriptor   ; bRequest=0x06
ajmp    EndOfRequestTable

inc     DPS
acall   SetDescriptor   ; bRequest=0x07
ajmp    EndOfRequestTable

inc     DPS
acall   GetConfiguration; bRequest=0x08
ajmp    EndOfRequestTable

inc     DPS
acall   SetConfiguration; bRequest=0x09
ajmp    EndOfRequestTable

inc     DPS
acall   GetInterface    ; bRequest=0x0A
ajmp    EndOfRequestTable

inc     DPS
acall   SetInterface    ; bRequest=0x0B
ajmp    EndOfRequestTable

inc     DPS
acall   SyncFrame       ; bRequest=0x0C
ajmp    EndOfRequestTable

```

```

BadRequest:
inc     DPS
acall   ZeroStall

```

EndOfRequestTable:

```

;; restore all registers
pop     ACC
mov     R0, A
pop     B
pop     DPL0
pop     DPL1
pop     DPH0
pop     DPH1
pop     DPS
pop     ACC
reti

```

```

;; -----
;;
;; ClearDataToggles
;;
;; Clears all of the data toggles and prepares for transfer
;;

```

```

ClearDataToggles:
;; we need to clear the data toggles on the EP we use
;; EP1OUT and EP1IN

```

```

;;
mov     DPTR, #TOGCTL
mov     A, #0b00000010 ; EP1OUT
movx    @DPTR, A
setb    ACC.5
movx    @DPTR, A

mov     A, #0b00010010 ; EP1IN
movx    @DPTR, A
setb    ACC.5
movx    @DPTR, A
ret

;; 888888888888888888888888888888888888888888888888888888888888888888888888888888888888888888888888888
;;
;; Request Handlers
;;
;;
;; -----
;;
;; -- Clear Feature
;;
;; We don't have remote wakeup so we don't have to handle that
;; feature. All we need to do here is clear stalled EP
;;

ClearFeature:
mov     DPTR, #SETUPDAT
movx    A, @DPTR
jz      clrftr_ret
cjne    A, #2, ZeroStall_jump

inc     DPTR
movx    A, @DPTR
cjne    A, #0x01, ZeroStall_jump

inc     DPTR
movx    A, @DPTR
jnz     ZeroStall_jump

mov     DPTR, #SETUPDAT+4
movx    A, @DPTR ; load A with EP# that is to be unstalled

mov     C, ACC.7
anl    A, #0x07 ; only need low 3 bits
jz     clrftr_ret ; we don't know what to do with EP0 (autoclear)
rl     A ; mul by two for proper offset address
jc     clr_in_ep ; ok, an in ep

mov     DPTR, #OUT1CS-2
acall  AddAtoDPTR
ajmp   clr_ep_now

clr_in_ep:
mov     DPTR, #IN1CS-2
acall  AddAtoDPTR

clr_ep_now:
movx    A, @DPTR ; clear the stall bit!
anl    A, #0b11111110
movx    @DPTR, A

clrftr_ret:
ret

;; -----
;;
;; -- GetConfiguration
;;

```

```

        ;; Gets the current configuration byte
GetConfiguration:
        ;; check if bmRequestType == 0x80
        mov     DPTR, #SETUPDAT
        movx   A, @DPTR
        mov     C, ACC.7
        jnc    ZeroStall_jump

        ;mov    DPTR, #cur_config
        ;movx  A, @DPTR      ; get cur config
        clr    A
        mov    DPTR, #IN0BUF
        movx   @DPTR, A      ; write it to ep0
        mov    DPTR, #IN0BC
        ;clr   A
        inc   A
        movx   @DPTR, A      ; set ep0 byte count to 1

getcfig_ret:
        ret

ZeroStall_jump:  ajmp     ZeroStall;half way point

        ;; -----
        ;;
        ;; GetDescriptor
        ;;
        ;; Loads the correct descriptor into the setup data pointer
        ;;
GetDescriptor:
        mov     DPTR, #SETUPDAT
        movx   A, @DPTR
        cjne   A, #0x80, ZeroStall_jump
; IN Device is the only one handled

        mov     DPTR, #SETUPDAT+3; Get Descriptor type dequest
        movx   A, @DPTR
        dec    A

        jz     getdescr_device
        dec    A
        jz     getdescr_config
        dec    A
        jz     getdescr_string
        ajmp   ZeroStall      ; huh? unkown req.

getdescr_device:
        mov     A, #>device_descriptor
        mov     DPTR, #SUDPTRH
        movx   @DPTR, A

        mov     A, #<device_descriptor
        mov     DPTR, #SUDPTRL
        movx   @DPTR, A

        ret

getdescr_config:
        mov     DPTR, #SETUPDAT+2
        movx   A, @DPTR
        jnz    ZeroStall_jump  ; only 1 configuration defined!!!

        mov     A, #>config0_descriptor
        mov     DPTR, #SUDPTRH
        movx   @DPTR, A

        mov     A, #<config0_descriptor

```

```

    mov     DPTR, #SUDPTRL
    movx   @DPTR, A

    ret

getdescr_string:
    mov     DPTR, #SETUPDAT+2
    movx   A, @DPTR

lolq:    cjne  A, #4+1, lolq
         jnc   ZeroStall_jump ; jump if string ref is > 4 [string we provide]

         mov   B, #13          ; 13 == size of each entry in the next jump table
         mul  ab
         mov  DPTR, #jump_string_table
         jmp  @A+DPTR
jump_string_table:
    ;; string 0
    mov     DPTR, #SUDPTRH ; len 3
    mov     A, #>string0_descriptor; len 2
    movx   @DPTR, A ; len 1

    mov     DPTR, #SUDPTRL
    mov     A, #<string0_descriptor
    movx   @DPTR, A
    ret                                         ; len 3+2+1+1=7

    ;; string 1
    mov     DPTR, #SUDPTRH ; len 3
    mov     A, #>string1_descriptor; len 2
    movx   @DPTR, A ; len 1

    mov     DPTR, #SUDPTRL
    mov     A, #<string1_descriptor
    movx   @DPTR, A
    ret                                         ; len 3+2+1+1=7

    ;; string 2
    mov     DPTR, #SUDPTRH ; len 3
    mov     A, #>string2_descriptor; len 2
    movx   @DPTR, A ; len 1

    mov     DPTR, #SUDPTRL
    mov     A, #<string2_descriptor
    movx   @DPTR, A
    ret                                         ; len 3+2+1+1=7

    ;; string 3
    mov     DPTR, #SUDPTRH ; len 3
    mov     A, #>string3_descriptor; len 2
    movx   @DPTR, A ; len 1

    mov     DPTR, #SUDPTRL
    mov     A, #<string3_descriptor
    movx   @DPTR, A
    ret                                         ; len 3+2+1+1=7

    ;; string 4
    mov     DPTR, #SUDPTRH ; len 3
    mov     A, #>string4_descriptor; len 2
    movx   @DPTR, A ; len 1

    mov     DPTR, #SUDPTRL
    mov     A, #<string4_descriptor
    movx   @DPTR, A
    ret                                         ; len 3+2+1+1=7

```

```

;; -----
;;
;; GetInterface
;;
;; Returns the current interface - that is 0
;;
GetInterface:
    mov     DPTR, #IN0BUF
    clr     A
    movx    @DPTR, A

    mov     DPTR, #IN0BC
    inc     A
    movx    @DPTR, A
    ret

;; -----
;;
;; SetDescriptor
;;
;; Don't do anything here. Just read the descriptor which we should
;; not have to read anyway
;;
SetDescriptor:
    ;; disarm the ep just if we actually have read it!
    mov     DPTR, #OUT0BC
    movx    @DPTR, A
    ret

;; -----
;;
;; SetConfiguration
;;
;; Sets the currently active configuration. But, we only use one!
;;
SetConfiguration:
    mov     DPTR, #SETUPDAT+2
    movx    A, @DPTR
    cjne    A, #0, ZeroStall_jump2

    acall   ClearDataToggles
    ret

;; -----
;;
;; SetFeature
;;
;; Stalls the appropriate EP and clears that EP's data toggles
;;
SetFeature:
    mov     DPTR, #SETUPDAT
    movx    A, @DPTR
    jz      setfeature_ret ; remote wakeup not supported anyway
    cjne    A, #0x02, ZeroStall_jump2; don't know the req.

    mov     DPTR, #SETUPDAT+4
    movx    A, @DPTR
    mov     C, ACC.7
    clr     ACC.7
    rl     A
    jz      setfeature_stall_zero_ep
    jc      setfeature_stall_ep_in

```

```

;; we need to stall an OUT EP
mov     DPTR, #OUT1CS-2
acall  AddAtoDPTR
movx   A, @DPTR
orl    A, #1
movx   @DPTR, A          ; EP stalled

mov     DPTR, #SETUPDAT+4
movx   A, @DPTR
anl    A, #7
movx   @DPTR, A
setb   ACC.5
movx   @DPTR, A

mov     DPTR, #SETUPDAT+4
movx   A, @DPTR
rl     A
mov     DPTR, #OUT0BC
acall  AddAtoDPTR
movx   @DPTR, A          ; write to BC for out EP
ret

setfeature_stall_ep_in:
mov     DPTR, #IN1CS-2
acall  AddAtoDPTR
movx   A, @DPTR
mov     A, #1            ; set stall and clear BSY
movx   @DPTR, A          ; stall IN EP

mov     DPTR, #SETUPDAT+4; clear the toggles
movx   A, @DPTR
anl    A, #7
setb   ACC.4
movx   @DPTR, A
setb   ACC.5
movx   @DPTR, A
ret

setfeature_stall_zero_ep:
mov     DPTR, #EPOCS
movx   A, @DPTR
orl    A, #1
movx   @DPTR, A          ; stall EP 0

setfeature_ret:
ret

```

```

ZeroStall_jump2:
ajmp   ZeroStall

```

```

;; -----
;;
;; GetStatus
;;
GetStatus:
mov     DPTR, #SETUPDAT+0
movx   A, @DPTR
cjne   A, #0x80, getstatus_stall_ep

clr    A
ajmp   getstatus_ret

getstatus_stall_ep:
mov     DPTR, #SETUPDAT+4
movx   A, @DPTR
mov     C, ACC.7
clr    ACC.7

```

```

    jz     getstatus_ep0
    jc     getstatus_stall_in_ep; it's the IN ep we need

    mov    DPTR, #EP0CS
    rl     A                ; mul by 2
    acall  AddAtoDPTR      ; adds A to DPTR
    movx   A, @DPTR
    anl   A, #1
    ajmp  getstatus_ret

getstatus_ep0:                ; returns status of EPO
    mov    DPTR, #EP0CS
    movx   A, @DPTR
    anl   A, #1
    ajmp  getstatus_ret

getstatus_stall_in_ep:
    mov    DPTR, #EP0CS
    rl     A                ; mul by 2
    acall  AddAtoDPTR      ; adds A to DPTR
    movx   A, @DPTR
    anl   A, #1
    ajmp  getstatus_ret

getstatus_ret:
    mov    DPTR, #IN0BUF
    movx   @DPTR, A        ; status has to be in A cause it's moved to in0 buf here
    inc    DPTR
    clr    A                ; put zero in second byte
    movx   @DPTR, A

    mov    A, #2
    mov    DPTR, #IN0BC
    movx   @DPTR, A
    ret

;; -----
;;
;; SetInterface
;;
;; We set the interface by clearing some toggles
;;
SetInterface:
    acall  ClearDataToggles

;; now, we need to clear any things for the EP as needed
;; EP1 OUT and EP1 IN
    mov    DPTR, #IN1CS
    movx   A, @DPTR
    anl   A, #0b11111101
    movx   @DPTR, A

    mov    DPTR, #OUT1BC
    movx   @DPTR, A
    ret

;; -----
;;
;; SyncFrame
;;
;; sync frames - return current frame + 8
;;
SyncFrame:
    ;mov    DPTR, #SETUPDAT+4
    ;movx   A, @DPTR
    ;cjne   A, #0x88, ZeroStall

    mov    DPTR, #USBFRAMEL
    movx   A, @DPTR
    mov    DPTR, #IN0BUF
    movx   @DPTR, A

```



```

mov     DPTR, #USBFRAMEH
movx   A, @DPTR
mov     DPTR, #IN0BUF+1
movx   @DPTR, A

mov     A, #1
mov     DPTR, #IN0BC
movx   @DPTR, A
ret

clr     A
mov     B, A
mov     DPTR, #USBFRAMEL
movx   A, @DPTR
add     A, 25
;jnc   SyncFrame_skip
;inc   B
SyncFrame_skip:
mov     DPTR, #IN0BUF
movx   @DPTR, A
mov     DPTR, #USBFRAMEH
movx   A, @DPTR
add     A, B
anl    A, #0b00000111
mov     DPTR, #IN0BUF+1
movx   @DPTR, A
mov     DPTR, #IN0BC
mov     A, #2
movx   @DPTR, A
SyncFrame_ret:
ret

;; -----
;;
;; ZeroStall
;;
;; stalls ep0 due to some event or problem
;;
ZeroStall:
ret

mov     A, #1
mov     DPTR, #IN1BUF
movx   @DPTR, A
mov     DPTR, #IN1BC
movx   @DPTR, A

mov     DPTR, #EPOCS
movx   A, @DPTR
orl    A, #1
movx   @DPTR, A
ret

;; Now, we need to define some descriptor tables here
;; that will get returned. + some other things
.area DSEG (DATA)
cur_config:      .db      0
device_descriptor:
.db      18          ; descriptor size
.db      1          ; DEVICE Descriptor Type
.db      0x10       ; USB Spec Release Number
.db      0x01
.db      0xFF       ; our own class of device <lol>
.db      0xff       ; subclass
.db      0xff       ; protocol
.db      64         ; max packet size for EP0
.db      0x3f       ; Vendor ID (0xff3f)
.db      0xff

```

```

        .db      10          ; product id
        .db      0
        .db      10          ; device id
        .db      0
        .db      1          ; 1 manufacturer string descriptor
        .db      2          ; 2 product string descriptor
        .db      3          ; 3 serial number string descriptor
        .db      1          ; num of configurations possible

config0_descriptor:
        .db      9          ; length
        .db      2          ; CONFIGURATION Descriptor Type
        .db      39         ; total length of this configuration (9+9+3*7)
        .db      0
        .db      1          ; num of interfaces
        .db      1          ; config num for this interface
        .db      4          ; 4 string descriptor for this config
        .db      0b10000000 ; config characteristics
        .db      51         ; 102 mA of power consumption

interface0_descriptor:
        .db      9          ; length
        .db      4          ; INTERFACE Descriptor Type
        .db      0          ; interface num
        .db      0          ; alternate setting number
        .db      3          ; num of end points
        .db      0xff       ; interface class
        .db      0xff       ; sub class
        .db      0xff       ; interface protocol
        .db      0          ; Interface string descriptor (null)

endpoint1out:
        .db      7          ; bulk out EP1 descriptor
        .db      5          ; length
        .db      5          ; EP Descriptor Type
        .db      1          ; OUT EP1
        .db      0x02       ; bulk type
        .db      16         ; 16 byte data requests are sent here
        .db      0
        .db      0          ; polling interval - ignored here

endpoint1in:
        .db      7          ; length
        .db      5          ; EP Descriptor Type
        .db      0b10000001 ; IN EP1
        .db      0x02       ; bulk type
        .db      64         ; 64 byte request responses returned here
        .db      0
        .db      0          ; polling interval - ignored here

endpoint8in:
        .db      7          ; length
        .db      5          ; EP Descriptor Type
        .db      0b10001000 ; IN EP8 ISO
        .db      0x01       ; ISO EP
        .db      144        ; max packet size to 400 (333 channels for min dwell time of
3us)
        .db      1
        .db      1          ; polling interval (1ms) for ISO stuff

string0_descriptor:
        .db      4          ; Lang table descriptor (EN only here)
        .db      3          ; len
        .db      3          ; STRING Descriptor Type
        .db      9          ; EN Lang
        .db      0

string1_descriptor:
        .db      10         ; manufacturer
        .db      10         ; len
        .db      3          ; STRING Descriptor Type
        .db      65         ; 'Adam'
        .db      0

```

```

        .db      100
        .db      0
        .db      97
        .db      0
        .db      109
        .db      0
string2_descriptor:      ; product
        .db      18      ; len
        .db      3      ; STRING Descriptor Type
        .db      65      ; Analyzer
        .db      0
        .db      110
        .db      0
        .db      97
        .db      0
        .db      108
        .db      0
        .db      121
        .db      0
        .db      122
        .db      0
        .db      101
        .db      0
        .db      114
        .db      0
string3_descriptor:      ; serial
        .db      8      ; len
        .db      3      ; STRING Descriptor Type
        .db      48      ; 0.1
        .db      0
        .db      46
        .db      0
        .db      49
        .db      0
string4_descriptor:      ; config descriptor
        .db      12      ; len
        .db      3      ; STRING Descriptor Type
        .db      66      ; Betsy
        .db      0
        .db      101
        .db      0
        .db      116
        .db      0
        .db      115
        .db      0
        .db      121
        .db      0

```